ENVISAT GOMOS Monthly report: September 2003

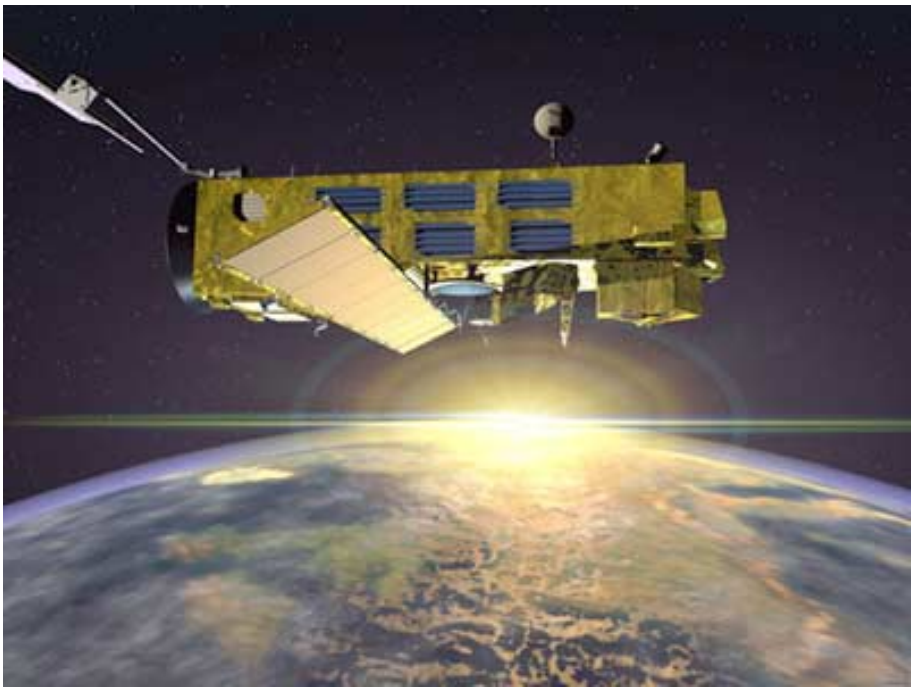

Prepared by:	PCF team	ESA EOP-GOQ
Inputs from:	GOMOS Quality Working Group	
Issue:	1.0	
Reference:	ENVI-SPPA-EOPG-TN-03-0021	
Date of issue:	20 Oct. 03	
Status:	Reviewed	
Document type:	Technical Note	
Approved by:	Pascal Lecomte, Rob Koopman	

TABLE OF CONTENTS

1 INTRODUCTION

The GOMOS monthly report documents the current status and recent changes to the GOMOS instrument, its data processing chain, and its data products.
The Monthly Report (hereafter MR) is composed of analysis results obtained by the Product Control Facility, combined with inputs received from the different entities working on GOMOS operation, calibration, product validation and data quality. These teams participate in the GOMOS Quality Working Group:

- European Space Agency (ESRIN-PCF, ESOC, ESTEC-PLSO)
- ACRI
- Service d'Aeronomie
- Finnish Meteorological Institute
- IASB-Belgian Institute for Space Aeronomy
- Atrium Space
- ECMWF

In addition, the group interfaces with the Atmospheric Chemistry Validation Team.

1.1 Scope

The main objective of the Monthly Report is to give, on a regular basis, the status of GOMOS instrument performance, data acquisition, results of anomaly investigations, calibration activities and validation campaigns. The following six sections compose the MR:

- Summary
- Unavailability
- Instrument Performance and Configuration
- Level 1 Product Quality Monitoring
- Level 2 Product Quality Monitoring
- Validation Activities and Results

1.2 References

[1] ENVISAT Weekly Mission Operations Report #67, #68, #69 ENVI-ESOC-OPS-RP-1011-TOS-OF
[2] 'Level 1b Detailed Processing Model', PO-RS-ACR-GS-0001, issue 5.4, 20 Nov, 2002
[3] 'Level 2 Detailed Processing Model', PO-RS-ACR-GS-0002, issue 5.4, 20 Nov, 2002

1.3 Acronyms and abbreviations

ACVT	Atmospheric Chemistry Validation Team
ADF	Auxiliary Data File
ADS	Auxiliary Data Server

ANX	Ascending Node Crossing
ARF	Archiving Facility (PDS)
CNES	Centre National d'Études Spatiales
CTI	Configurable Transfer Item
CR	Cyclic Report
DC	Dark Charge
DMOP	Detailed Mission Operation Plan
DPM	Detailed Processing Model
DS	Data Server
DSA	Dark Sky Area
DSD	Data Set Descriptor
ECMWF	European Centre for Medium Weather Forecast
EQSOL	Equipment Switch Off Line
ESA	European Space Agency
ESRIN	European Space Research Institute
ESTEC	European Space Research & Technology Centre
ESOC	European Space Operations Centre
FCM	Fine Control Mode
FMI	Finnish Meteorological Institute
FP1	Fast Photometer 1
FP2	Fast Photometer 2
GOMOS	Global Ozone Monitoring by Occultation of Stars
GOPR	GOmos PRototype
GS	Ground Segment
HK	Housekeeping
IASB	Institut d'Aeronomie Spatiale de Belgique
IAT	Interactive Analysis Tool
ICU	Instrument Control Unit
IDL	Interactive Data Language
IECF	Instrument Engineering and Calibration Facilities
IMK	Institute of Meteorology Karlsruhe (Meteorologisch Institut Karlsuhe)
INV	Inventory Facilities (PDS)
IPF	Instrument Processing Facilities (PDS)
JPL	Jet Propulsion Laboratory
LAN	Local Area Network
LPCE	Laboratoire de Physique et Chimie de l'Environnement
LUT	Look Up Table
MCMD	Macro Command
MDE	Mechanism Drive Electronics
MIP	Most Illuminated Pixel
MPH	Main Product Header
MR	Monthly Report
OCM	Orbit Control Manoeuvre
OOP	Out-of-plane
OP	Operational Phase of ENVISAT
PAC	Processing and Archiving Centre (PDS)
PCF	Product Control Facility
PDCC	Payload Data Control Centre (PDS)

PDHS	Payload Data Handling Station (PDS)
PDHS-E	Payload Data Handling Station – ESRIN
PDHS-K	Payload Data Handling Station – Kiruna
PDS	Payload Data Segment
PLSOL	Payload Switch off Line
PMC	Payload Module Computer
PRNU	Pixel Response Non Uniformity
QC	Quality Control
QUARC	Quality Analysis and Reporting Computer
QWG	Quality Working Group
RIVM	Rijksinstituut voor Volksgezondheid en Milieu
RTS	Random Telegraphic Signal
SA	Service d'Aeronomie
SATU	Star Acquisition and Tracking Unit
SFCM	Stellar Fine Control Mode
SFM	Steering Front Mechanism
SMNA	Servicio Meteorológico Nacional de Argentina
SODAP	Switch On and Data Acquisition Phase
SPA1	Spectrometer A CCD 1
SPA2	Spectrometer A CCD 2
SPB1	Spectrometer B CCD 1
SPB2	Spectrometer B CCD 2
SPH	Specific Product Header
SQADS	Summary Quality Annotation Data Set
SSP	Sun Shade Position
SZA	Solar Zenith Angle

2 SUMMARY

The GOMOS instrument has been operating nominally during the month of September. It had three unavailability periods during the month that were not critical for the mission (section 3.1).

The availability of level 1b data within the archives increased until 98.5 % during the last week of September. The level 0 availability was 100% during the last two weeks of the month (section 3.3).

The temperature behaviour of the detectors is nominal within the reporting period. The expected seasonal variation of the temperatures with amplitude of around one degree can be observed (section 4.2).

The elevation at which stars first appear on the star tracking detector shows significant deviation in elevation from the expected position. Stars now initially appear above the SATU centre. The variation in this MIP positions displays seasonal variation and is an indicator of an ENVISAT platform attitude problem (section 4.5.3).

The variation of the radiometric sensitivity ratio is outside the threshold for some photometer ratios. Investigation results will be reported in future monthly reports (section 5.4.1).

On 9th, 19th and 29th September 2003 new calibration ADF's were disseminated with updated DC map of orbits 07955, 08111 and 08253 respectively.

ESA has continued the supply of selected data products to validation teams using the prototype processor at ACRI. An upgrade of the data processing algorithm specification is in progress, in order to improve both level 1 and level 2 products.

3 INSTRUMENT UNAVAILABILITY

3.1 GOMOS unavailability periods

In table 3.1-1 there is a list of GOMOS unavailability reports issued during the period 1st September (00:00:00) 2003 until 30th September (24:00:00) 2003.

- The first unavailability period occurred on 4th September when an anomaly related to a known PMC software problem caused the switch down of all ENVISAT payload instruments. GOMOS was again in operation on 6th September at 18:22.

- On 8th September at 04:24 GOMOS went to Heater/Refuse after a "failed_centering" anomaly. The star id 162 was centered well and then the transition to tracking failed. A potential cause currently under investigation is the star weakness (just under the limit of the criteria threshold). This star 162 was successfully tracked some hours before so the conditions of straylight might also be in cause. The anomaly was considered uncritical and GOMOS was back to measurement on 8th September at 20:47.

- GOMOS autonomously was switched to Reset/Wait on Saturday, 13th Sept. Analysis of PMC reporting has shown a MCMD Transfer Acknowledge Error at 09:45 to trigger the EQSOL/ICU Suspend. After a complete memory dump, GOMOS was recovered successfully on 16th September.

Table 3.1-1 List of unavailability reports issued during September

Reference of unavailability report	Start time Star orbit	Stop time Stop orbit	Description
EN-UNA-2003/0257	4 Sep 2003 22:52:52.000 Day of Year = 247 Orbit = 07914 Anx Offset = 0437.199	6 Sep 2003 18:22:54.000 Day of Year = 249 Orbit = 07940 Anx Offset = 0105.071	Recovered from PLSOL in Occultation.
EN-UNA-2003/0262	8 Sep 2003 04:24:57.000 Day of Year = 251 Orbit = 07960 Anx Offset = 1909.511	8 Sep 2003 20:47:25.000 Day of Year = 251 Orbit = 07970 Anx Offset = 0498.231	Failed centering anomaly. GOMOS recovered in Occultation.
EN-UNA-2003/0274	13 Sep 2003 09:45:53.000 Day of Year = 256 Orbit = 08035 Anx Offset = 0470.911	16 Sep 2003 21:36:36.000 Day of Year = 259 Orbit = 08085 Anx Offset = 0517.511	GOMOS autonomously was switched to Reset/Wait.

3.2 Stars lost in centering

The acquisition of a star initiates with a rallying phase where the telescope mechanism is directed towards the expected position of the star. Subsequently the acquisition procedure enters into detection mode, where the SATU star tracker output signal is pre-processed for spot presence survey and for the location of the most illuminated couple of adjacent pixels for two added lines, over the detection field. The Most Illuminated Pixel (MIP) defines the position of the first SATU centering window. The next step in the acquisition sequence is then initiated and consists of a centering phase where the SATU output signal is pre-processed for spot presence survey over the maximum of 10x10 pixel field. This allows the third phase to begin: the tracking phase.
The centering phase has occasionally resulted in loss of the star from the field of view. The fig. 3.2-1 reports the percentage of the stars lost in centering for the period 03-FEB-2003 to 28-SEP-2003. It can be seen that some stars, mainly weak stars (higher star id means higher magnitude) are lost during centering phase in more than 5% of their planned observations. As the monitoring shows neither trend nor excessively high percentages of loss, there is no need for the moment to reject any star from the catalogue, and there is no indication of instrument-related problems.

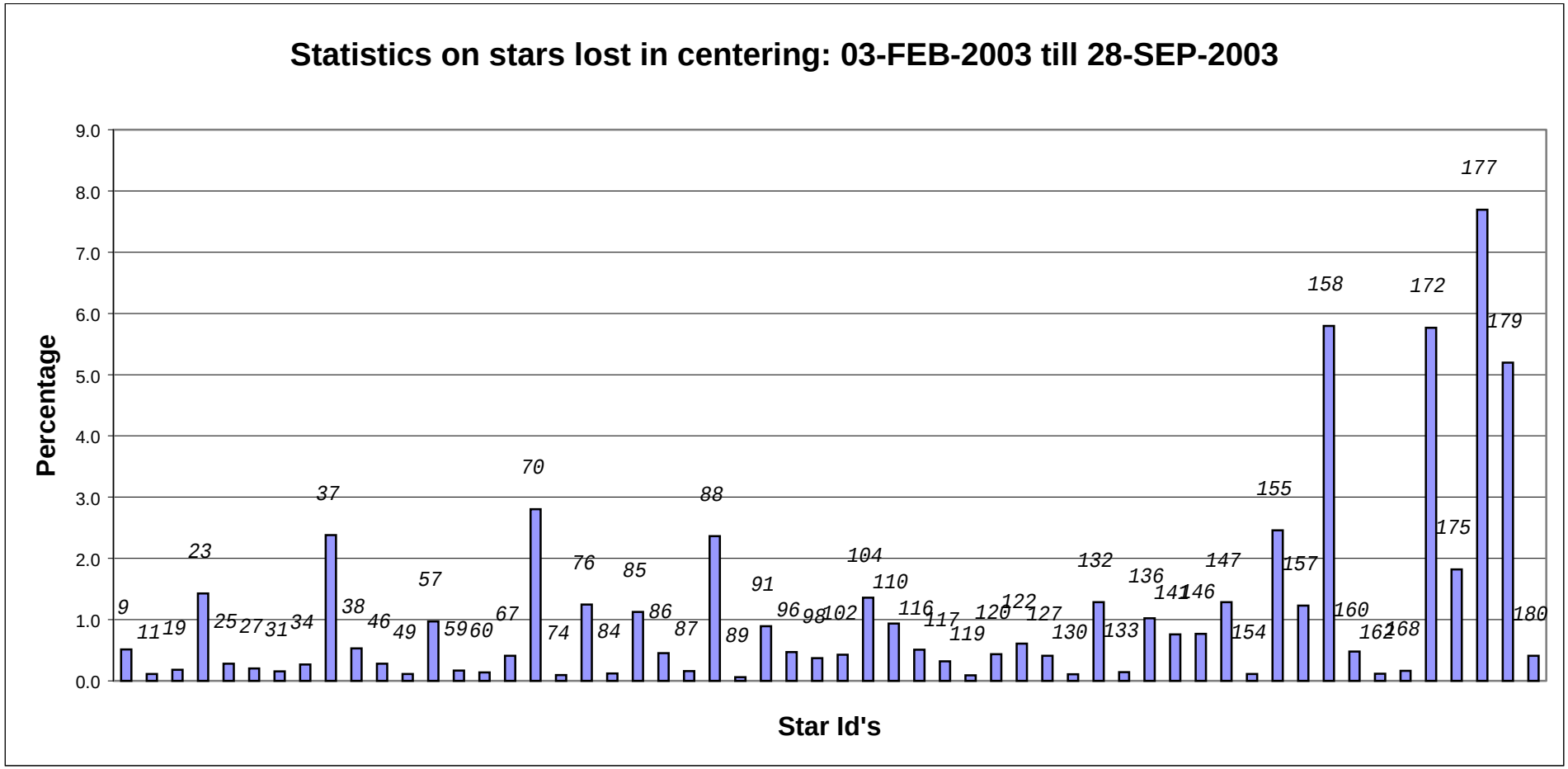

Figure 3.2-1: Statistics on stars that have been lost during the centering phase. The numbers above the columns correspond to the Star Id's.

3.3 Data generation gaps

The trend in percentage of missing data within the archives PDHS-K and PDH-E is depicted in fig. 3.3-1 (when instrument was in operation). It is a good indicator on how the PDS chain is working in terms of generation and dissemination of data to the archives. The percentage is calculated once per week.

The missing level 1b data within the archives decreased till 1.5 % during the last week of September. Regarding the level 0 there are no missing data during the last two weeks of September even if at the beginning of the month it arrived to 8 % of missing.

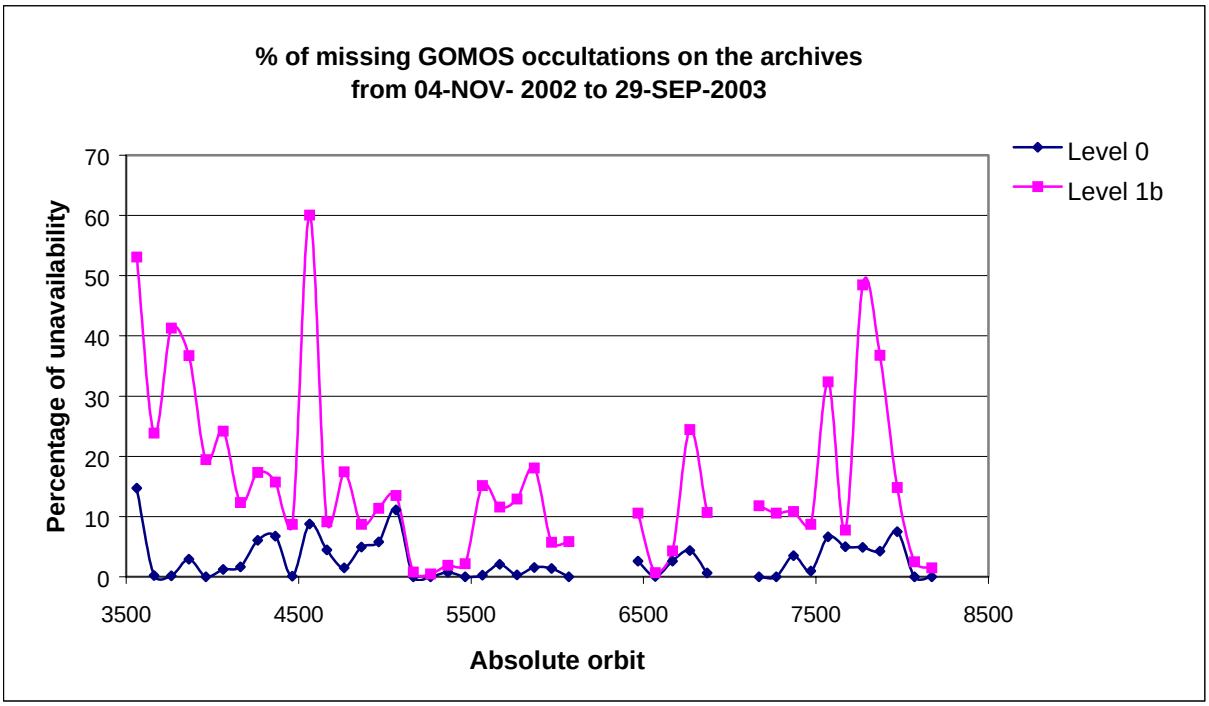

Figure 3.3-1: Percentage of level 0 and level 1b data missing on the archives PDHS-E and PDHS-K

3.3.1 GOM_NL__0P

Occultations planned to be acquired but for which no GOM_NL__0P data product has become available are presented in fig. 3.3-2 for the month of September 2003.

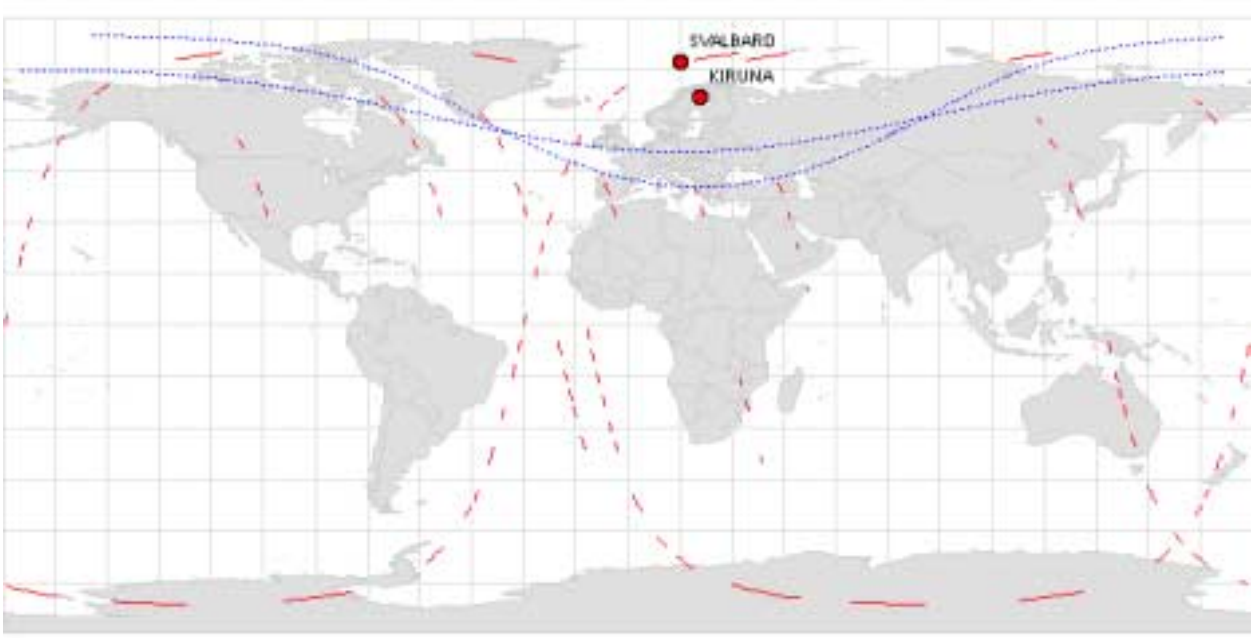

Figure 3.3-2: Orbit segments corresponding to planned data acquisitions for which no GOMOS level 0 product has become available

3.3.2 HIGHER-LEVEL PRODUCTS

Routine dissemination of higher-level products produced by the PDS to Cal/Val teams and other users has not yet begun. Currently ESA provides the Cal/Val teams with selected products that are generated with the prototype processor developed and operated by ACRI.

4 INSTRUMENT CONFIGURATION AND PERFORMANCE

4.1 Instrument Operation and Configuration

Since end of March the instrument has suffered some changes in the minimum azimuth range configuration in order to avoid the anomaly "Voice_coil_command_saturation" that caused the instrument to go into STAND BY/REFUSE mode. Since the change to the redundant chain B on July, the full range in azimuth has been again used (table 4.1-1).

Table 4.1-1: Historical changes in Azimuth configuration

Date	Orbit	Minimum Azimuth
29-MAR-2003 17:40	5635	0.0
31-MAY-2003 06:22	6530	+4.0
16-JUN-2003 16:17	6765	+12.0
15-JUL-2003 01:39	7200	-10.8

The operations of the instrument in other modes than occultation mode are identified in table 4.1-2.

There were no new Configurable Transfer Items (CTI) uploaded to the instrument. The file used is in table 4.1-3.

Table 4.1-2: GOMOS operations during September 2003

UTC time	Start orbit	Stop orbit	Mode (Asynchronous or Synchronous)	Calibration (CAL) or Dark Sky Area (DSA)
06 Sep 2003 06:36:51	7933	7940	A	CAL53
13 Sep 2003 07:57:20	8034	8034	A	DSA75
20 Sep 2003 07:37:13	8134	8134	A	DSA76
27 Sep 2003 07:17:06	8234	8234	A	DSA77

Table 4.1-3: CTI files for the reporting since July 2003

CTI files	Validity
CTI_SMP_GMVIEC20030716_123904_00000000_00000004_20030715_000000_20781231_235959.N1	20030715
CTI_SMP_GMVIEC20021104_075734_00000000_00000003_20021002_000000_20781231_235959	20021002

4.2 Thermal Performance

Since the beginning of the mission the hot pixel and RTS phenomena (see section 4.4.1) are producing a continuous increase of the dark charge signal within the CCD detectors. In order to minimize this effect, three successive CCD cool down were performed in orbits 800 (25th April 2002), 1050 (13th May 2002) and 2780 (11th September 2002).

Fig. 4.2-1 and 4.2-2 display, respectively, the overall temperature variation and the temperature variation around the Ascending Node Crossing (ANX) time with a resolution of 0.4 degrees (coding accuracy for level 0 data). The CCD temperatures during September are very similar to the ones registered in August. The expected seasonal variation of the temperatures with amplitude of around one degree can be clearly observed. The peaks that occur in spectrometer B1 and B2 are also to be noted. They happen a little before the ANX for some consecutive orbits and every 8-10 days. Their origin is still not known, as we did not find any correlation between these peaks and other activities carried out on the satellite. The CCD temperature at almost the same latitude location (fig. 4.2-2) is monitored in order to detect any inter-orbital temperature variation.

The decrease observed on 24th March and twice in September in all detectors is after GOMOS switch off periods, when the instrument did not have enough time to reach the nominal temperature before starting the measurements.

The orbital temperature variation of the detector SPB2 (fig. 4.2-3 for & 4.2-4) is bigger than nominal because GOMOS started to measure before reaching the nominal thermal configuration after the switch off periods. The maximum difference between ascending and descending passes was around 3.3 degrees. The stability of the temperature during the orbit is important because it affects the position of the interference patterns. The phenomenon of the interference is present mainly in SPB and this Pixel Response Non-Uniformity (PRNU) is corrected during the processing.

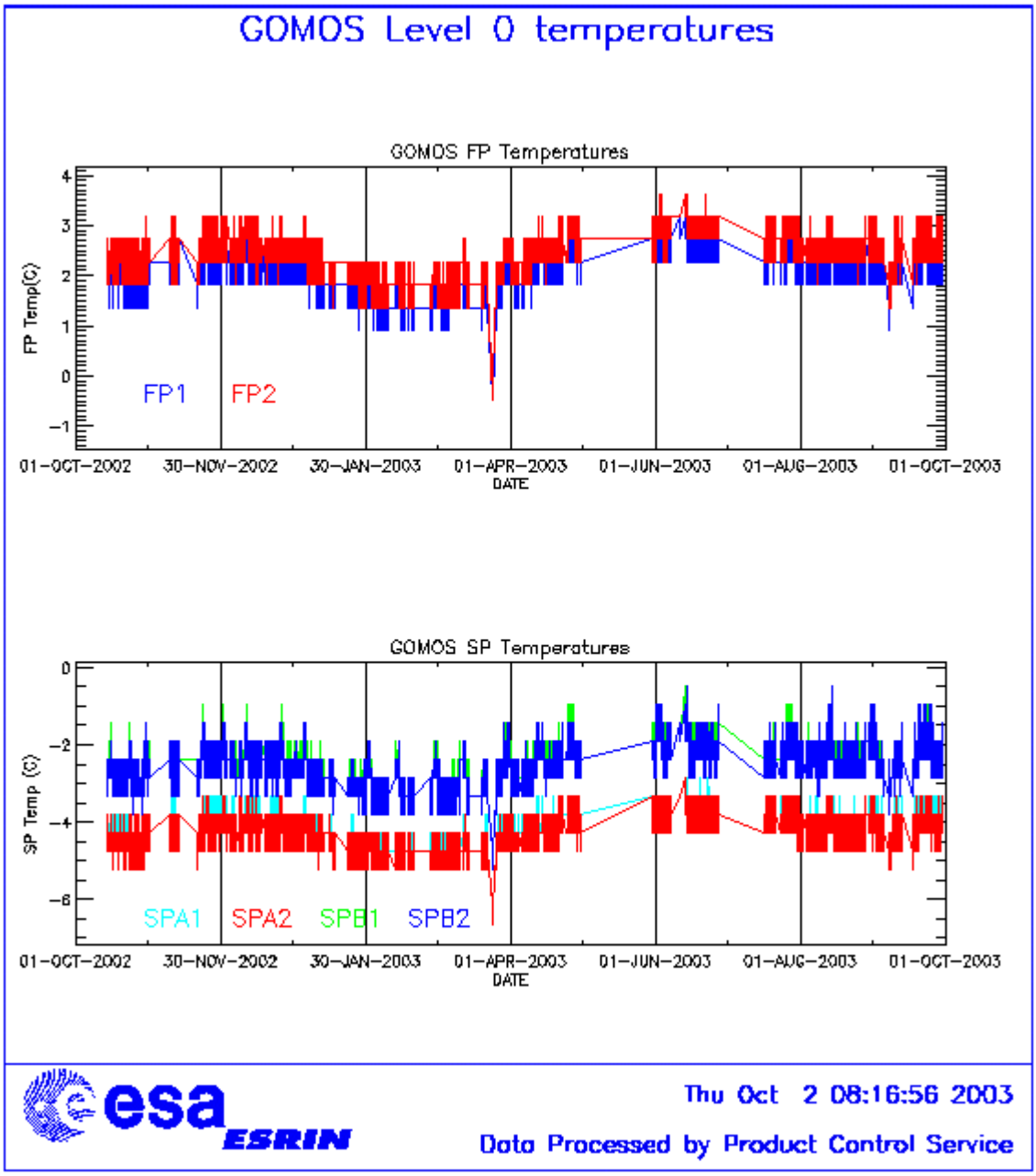

Figure 4.2-1: Level 0 temperature evolution of all GOMOS CCD detectors from October 2002 until end of September 2003

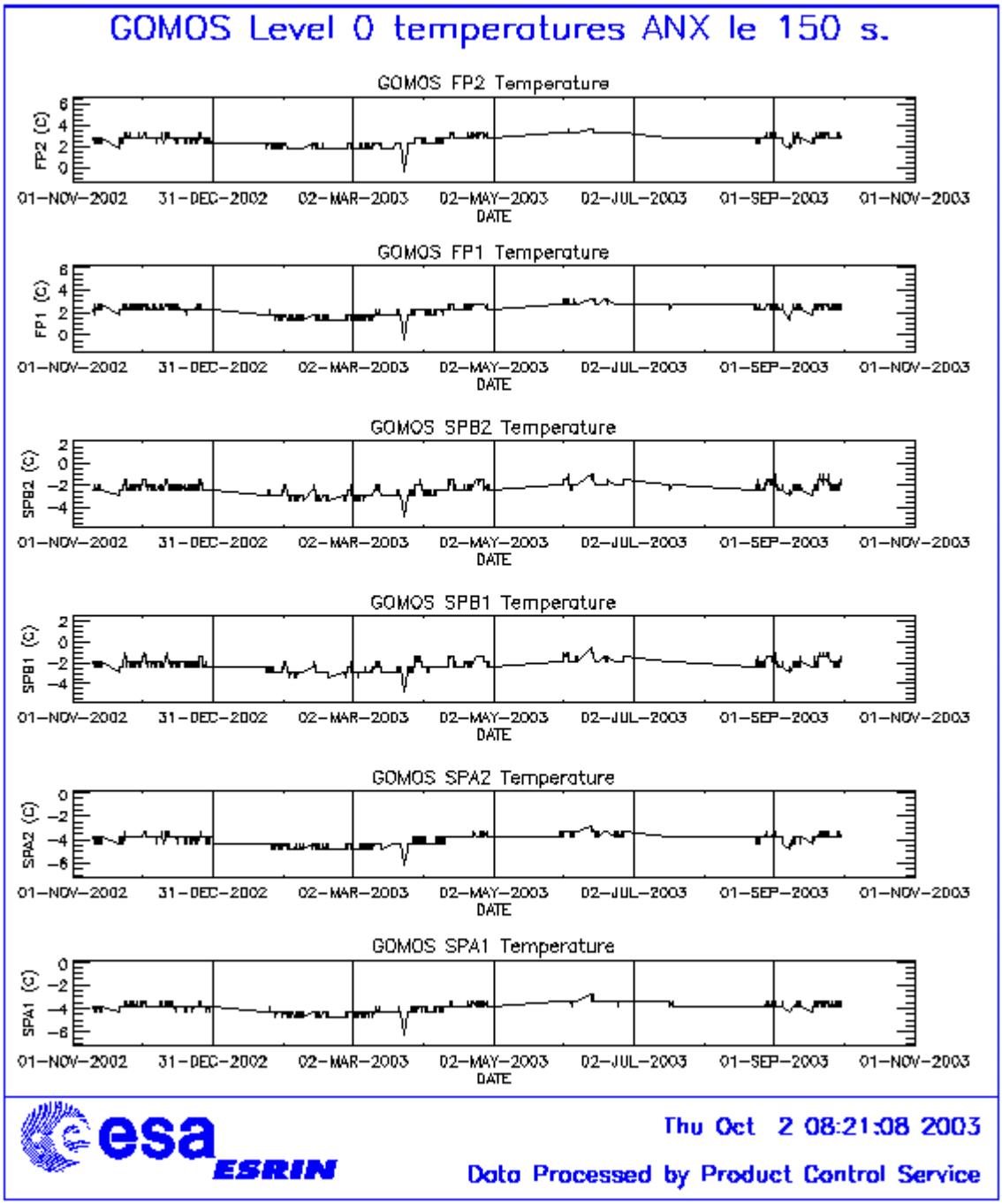

Figure 4.2-2: Level 0 temperature evolution of all GOMOS CCD detectors around ANX from November 2002 until end of September 2003

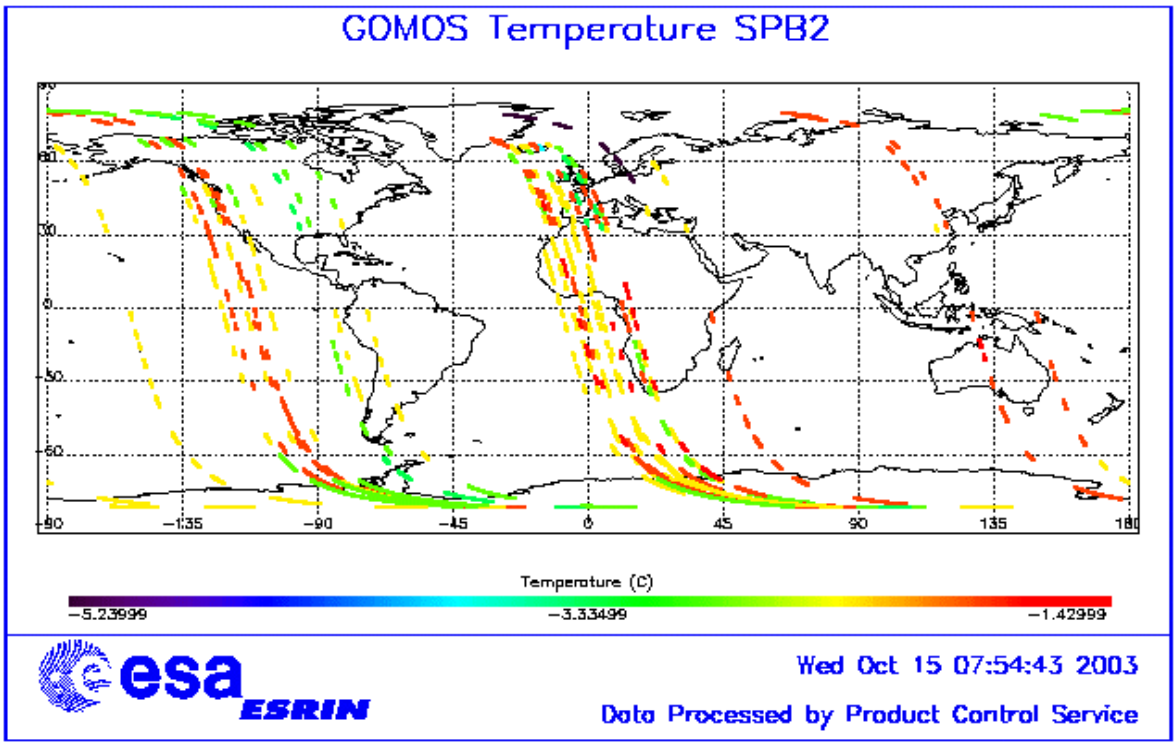

Figure 4.2-3: Ascending orbital variation of SPB2 temperature during some orbits on September 2003

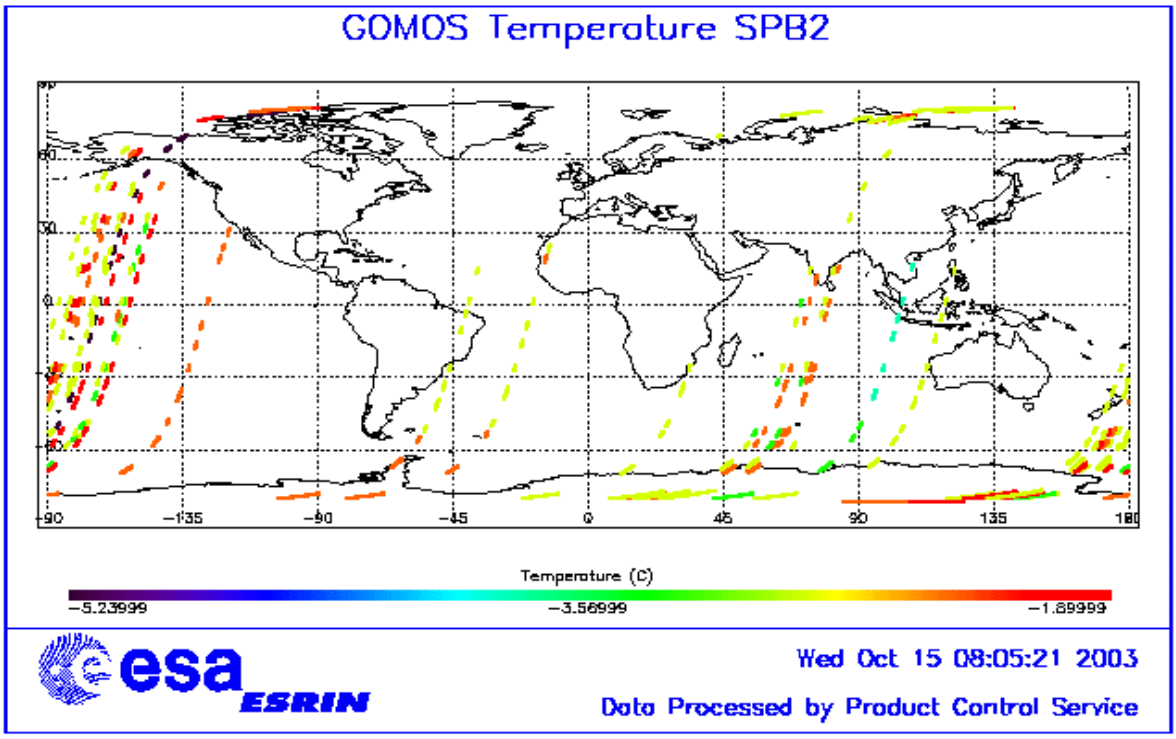

Figure 4.2-4: Descending orbital variation of SPB2 temperature during some orbits on September 2003

4.3 Optomechanical Performance

No new band setting calibration has been performed during September. These results were already presented in previous versions of the MR.

The position of stellar spectra of star id 2, 9 and 18 observed in dark-limb spatial spread monitoring mode have been averaged above 120 km altitude, and compared to the average positions before the transition to redundant chain on 15th July 2003 (blue dots in fig. 4-3.1). In table 4.3-1 the mean values of the location of the star signal for all the calibration analysis done till now are reported. The 'left' and 'right' values are calculated (the whole interval is not used) because the spectra present a slight slope, more pronounced in the spectrometer B (see fig. 4-3.1). The current processors GOMOS IPF 4.00 and GOPR prototype 5.4 still expect the spectra to be aligned along CCD lines, and therefore use only a single average line index per CCD. The values currently implemented of 81, 80, 82, 82 for SPA1, SPA2, SPB1 and SPB2 are still compatible with the observed 'left' and 'right' average position. The lookup table implemented in the version 6.0 of the prototype level 1 processor has been updated in order to have the line index as a function of the wavelength.
In table 4.3-2, mean values of the location of the star signal are calculated for some specific wavelength intervals. These intervals have been changed between the calibration performed in September 2002 and the ones performed afterwards. The results obtained are very similar to the ones obtained in previous exercises.
Table 4.3-3 reports the average location of the star spot on the photometer 1 and 2 CCD. No difference has been found for both photometers in column and in row positions.

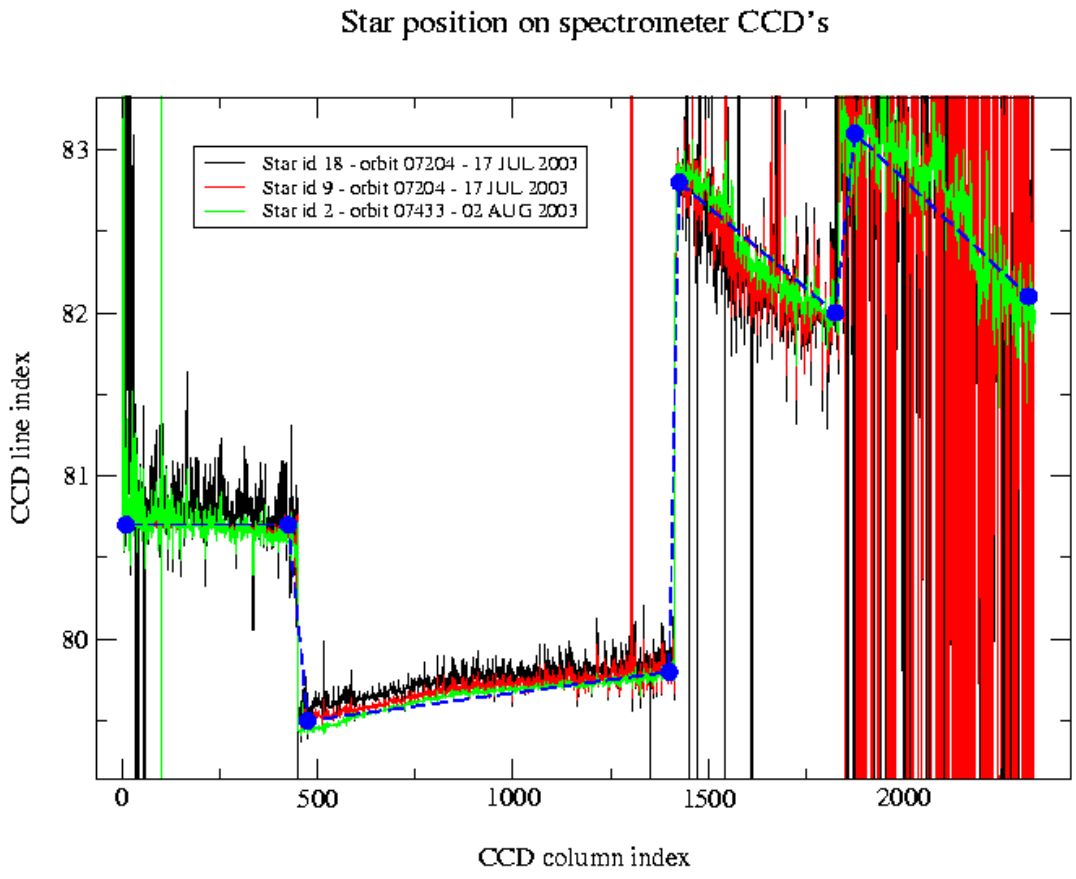

Figure 4.3-1: Average position of star spectra on the CCD

Table 4.3-1: Mean value of the location of the star signal during the occultation at the edges of every band (mean over 50 values, filtering the outliers)

	UV (SPA1) left/right	VIS (SPA2) left/right (Inverted spectra)	IR1 (SPB1) left/right	IR2 (SPB2) left/right
11/09/2002	80.7/80.7	79.8/79.5	82.8/81.9	83.1/82.1
01/01/2003	80.7/80.6	79.8/79.5	82.8/82.0	83.2/82.2
17/07/2003 & 02/08/2003	80.7/80.7	79.8/79.5	82.8/81.9	83.1/82.1

Table 4.3-2: Mean value of the location of the star signal during the occultation (as table 4.3-1) but now within some wavelength intervals

	UV (SPA1)	VIS (SPA2)	IR1 (SPB1)	IR2 (SPB2)
11/09/2002 wl range (nm)	80.8 [300-330]	79.8 [500-530]	82.6 [760-765]	82.9 [937-942]
01/01/2003 wl range (nm)	80.6 [350-360]	78.6 [650-670]	81.6 [760-765]	80.3 [935-945]
02/08/2003	80.7	79.9	82.3	

Table 4.3-3: Average column and row pixel location of the star spot on the photometer CCD during the occultation

	FP1 (column/row)	FP2 (column/row)
11/09/2002	11/4	5/5
01/01/2003	10/4	6/4.9
02/08/2003	10/4	6/5

4.4 Electronic Performance

4.4.1 DARK CHARGE EVOLUTION AND TREND

The trend of Dark Charge (DC) is of crucial importance for the final quality of the products, and is therefore subject to intense monitoring. As part of the DC there is:

- "Hot pixels", a pixel is "hot" when its dark charge exceeds its value measured on ground, at the same temperature, by a significant amount.
- RTS phenomenon (Random Telegraphic Signal), it is an abrupt change (positive or negative) of the CCD pixel signal, random in time, affecting only the DC part of the signal and not the photon generated signal.

The temperature dependence of the DC would make this parameter a good indicator of the DC behaviour, but the hot pixels and the RTS are producing a continuous increase of the DC (see trend in fig. 4.4-1 and 4.4-2). To take into account these phenomena, in the last version of the level 1 processor (GOMOS/4.00) operational since May 2003, a DC map per orbit is extracted from a Dark Sky Area (DSA) observation performed around ANX (full dark conditions). For every level 1b product (occultation), the actual thermistor temperature of the CCD is used to convert the DC map measured around ANX into an estimate of the DC at the time (and different temperature) of the

actual occultation. When the DSA observation is not available, the DC map inside the calibration product that was measured at a given thermistor reference temperature is used; again, the actual thermistor temperature of the CCD is used to compute the actual map.

In fig. 4.4-1 and 4.4-2 it is plotted the average DC inserted by the processor into the level 1b data products for the spectrometers SPA1 and SPB1 (per band: upper, central and lower). From the figures, it can be noted that the rate of increase of DC for the last four months is different from the previous months. Since the beginning of February till beginning of June the increase in SPA2 was around 350 electrons whilst since June to beginning of October the increase was around 100 electrons.

The same DC values are plotted in fig. 4.4-3 but for some occultations only during the reporting period.

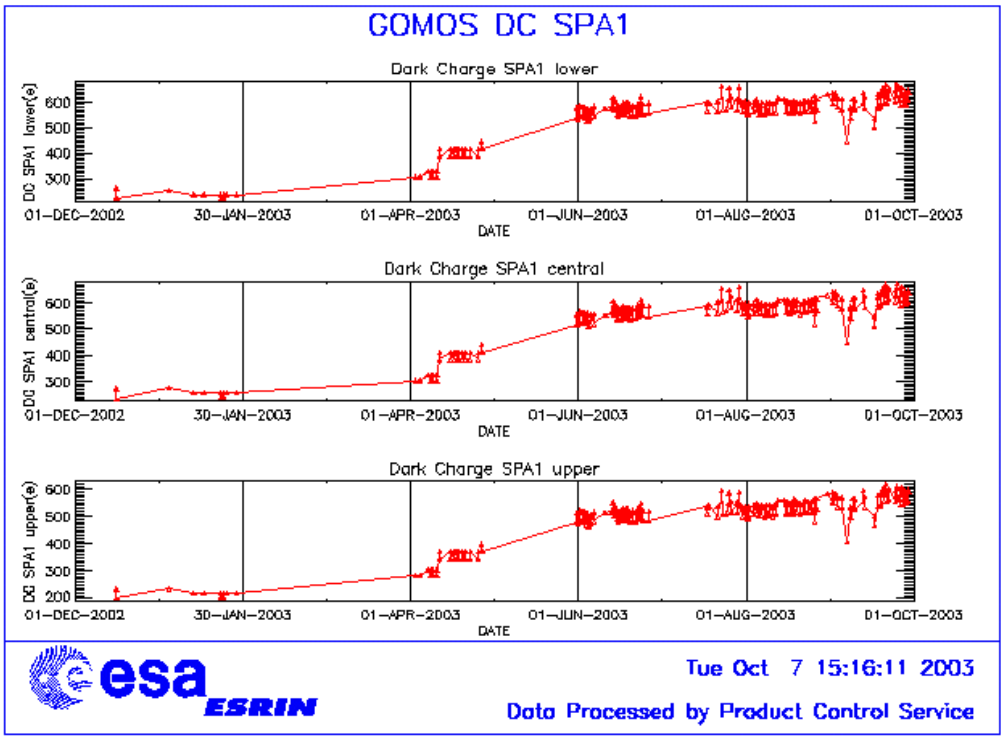

Figure 4.4-1: Mean DC evolution on SPA1 from 15th December 2002 until end of September 2003

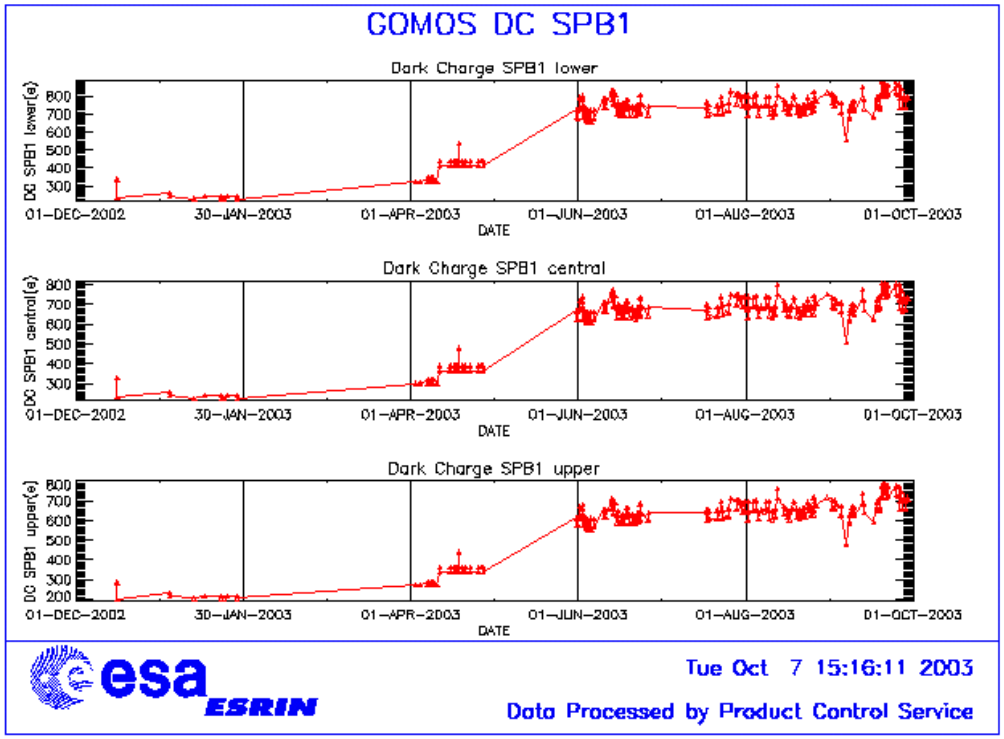

Figure 4.4-2: Mean DC evolution on SPB1 from 15th December 2002 until end of September 2003

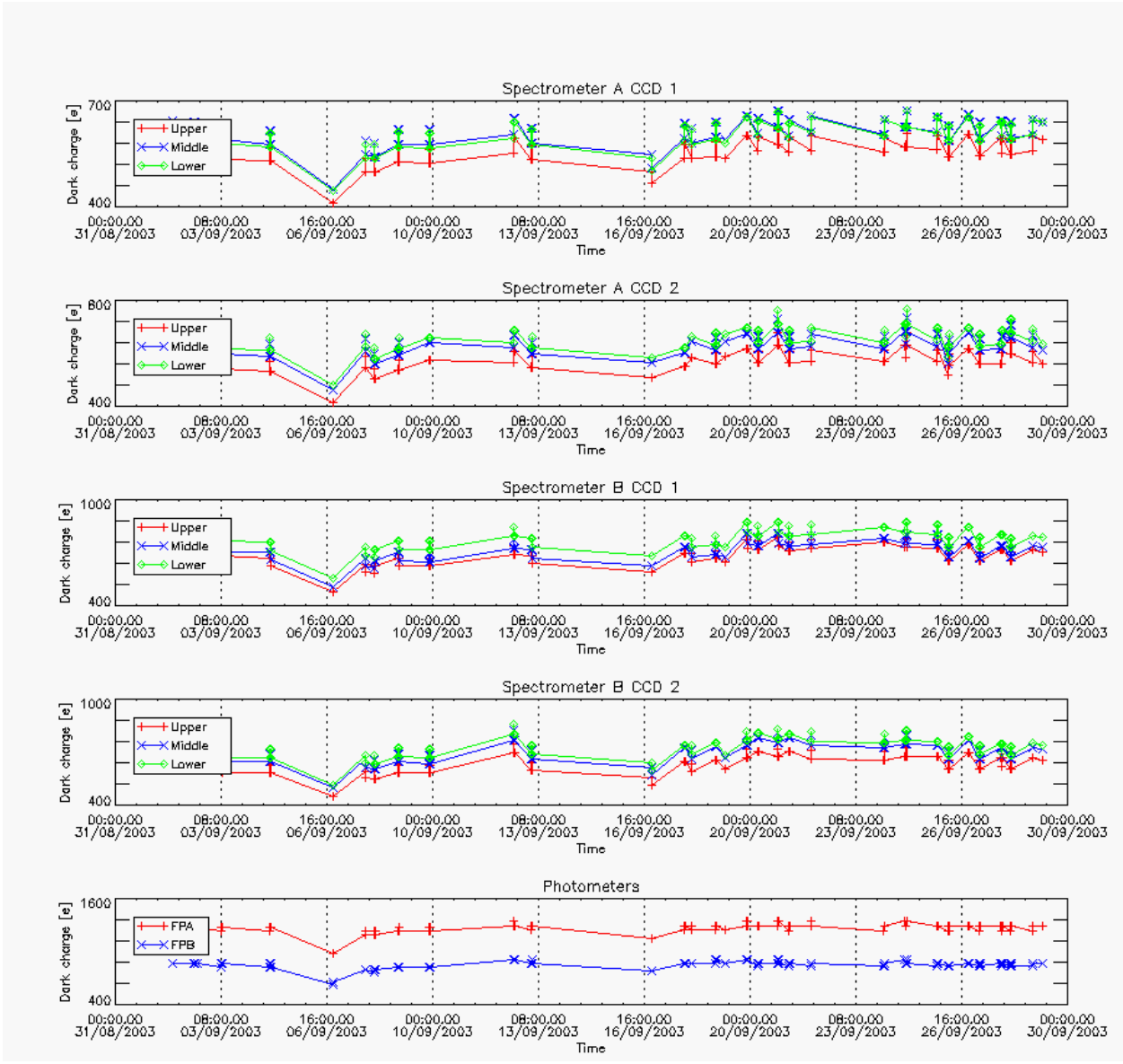

Figure 4.4-3: Mean Dark Charge of spectrometers and photometers during September2003

4.4.2 SIGNAL MODULATION

A parasitic signal was found to be systematically present, added to the useful signal, at least for spectrometers A1 and A2. The modulation is corrected in the data processing, but the modulation signal standard deviation is routinely monitored in order to detect any trend (fig. 4.4-4).

The modulation standard deviation, for every spectrometer, is characterised as follows:

$$\sigma_{mod} = (\text{'static noises'} - \text{'total static variance'})^{1/2} / \text{gain} \qquad \text{(in ADU)}$$

- The ‘static noises’ are calculated from the DSA observation performed once per orbit
- The ‘total static variance’ is obtained from ADF data (electronic chain noise, quantisation noise).

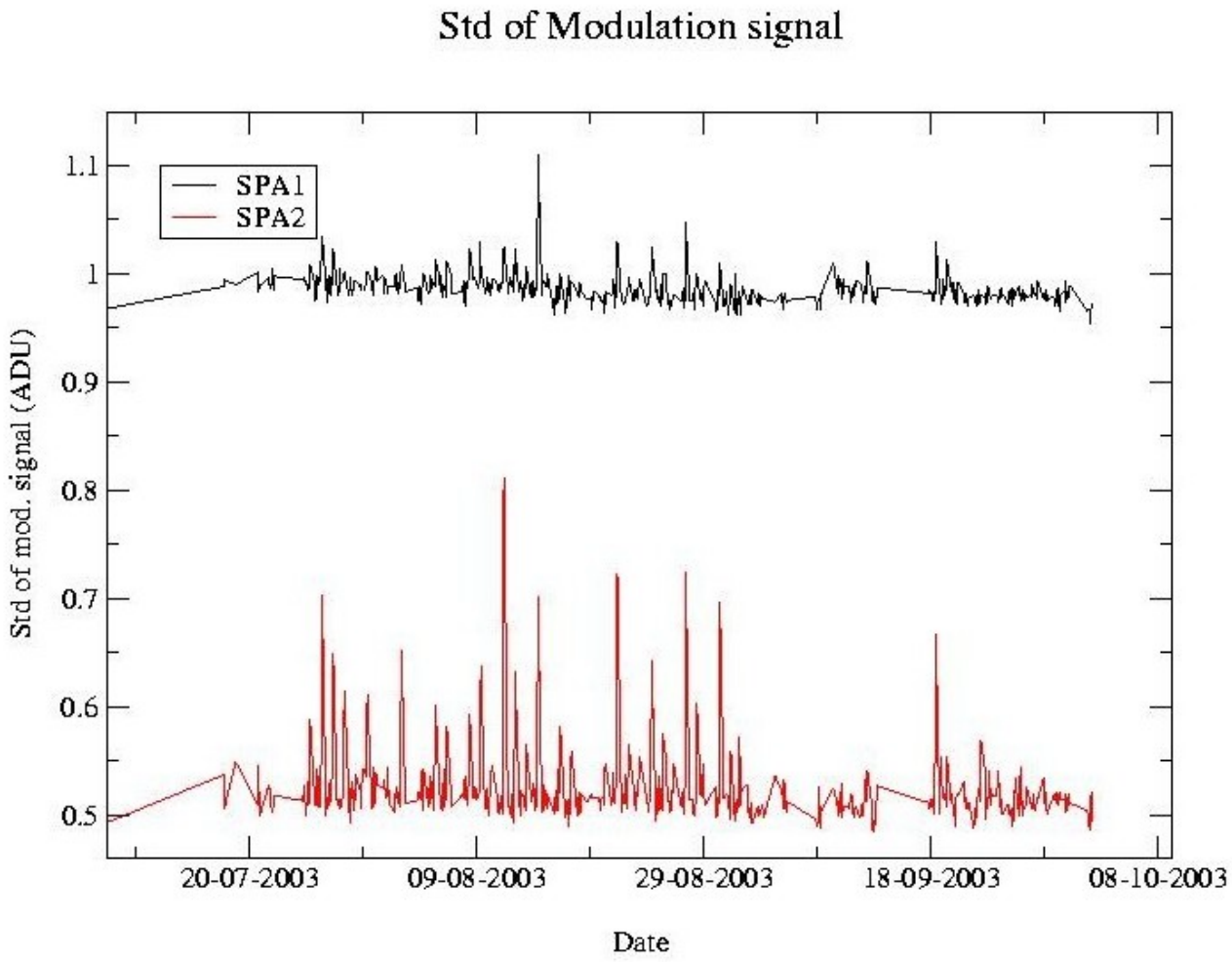

Figure 4.4-4: Standard deviation of the modulation signal

4.4.3 ELECTRONIC CHAIN GAIN AND OFFSET

No new electronic chain gain and offset calibration has been done during the reporting month so these results have been already presented in previous MR.

The routine monitoring of the ADC offset is a good indicator of the ageing of the instrument electronics. During the definition of this routine activity, an exercise has been done to analyse the variation of the ADC offset using the calibration observation in linearity mode (orbits 2810, 4384, 4834, 5219 and 5734).

The fig. 4.4-5 presents the evolution of the calibrated ADC offset for each spectrometer electronic chain. The unexpected increase of this offset seems to be due to an external contribution. In the ADC

offset calibration procedure, linearity observations are used with two integration times of 0.25 and 0.50 seconds to extrapolate to an integration time of 0 seconds that give the complete chain offset and not only the ADC offset. The complete offset contains any possible offsets, and especially the static dark charge (i.e. the dark charge that does not depend of the spectrometer integration time). If the memory area of the CCD is affected by the generation of hot pixels (this is confirmed by the presence of vertical lines visible in the measurement maps in spatial spread monitoring mode), it becomes that the increase observed in fig. 4.4-5 is due to these new hot pixels.

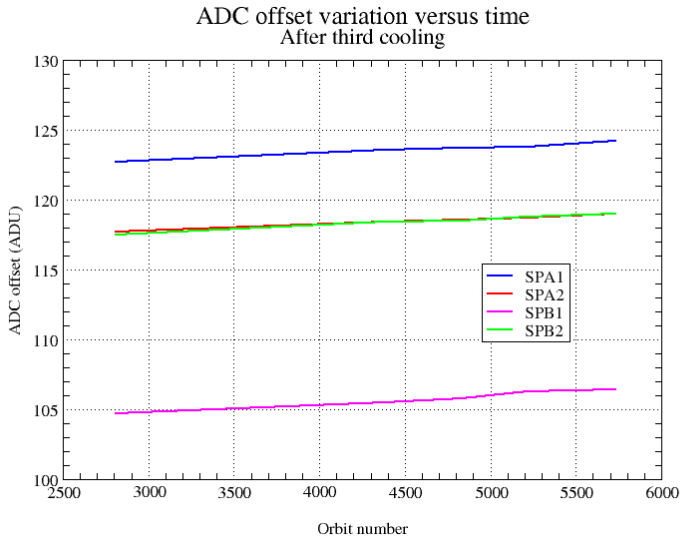

Figure 4.4-5: Evolution of the ADC offset for each spectrometer electronic chain

Next task consists in completing the analysis to confirm that the offset increase is due to the hot pixels in memory area. This can be proven by the study of the noise due to the increased dark charge. The increase of ADC offset will be assumed to be equal to the increase of 'static dark charge' and the corresponding noise will be computed and compared to the increase of the signal variance residual.

If we keep the ADC offset constant, as it is also used to compute the dark charge at band level used to correct the samples in the level 1b processing, the increase of the static dark charge - not taken into account in the ADC offset - is compensated by an artificial increase of the calibrated dark charge. So, the star and limb spectra are correctly corrected for dark charge. A small bias can be added to the instrument noise due to the incorrect dark charge level. Anyway, this quantity is not large enough to require a modification of the ADC offset value.

4.5 Acquisition, Detection and Pointing Performance

4.5.1 SATU NOISE AND EQUIVALENT ANGLE

The Star Acquisition and Tracking Unit (SATU) noise equivalent angle (SATU NEA) consists of the statistical angular variation of the SATU data above the atmosphere.

The mean of the standard deviation (std over the 50 values per measurement) above 105 km are computed for every occultation, giving two values per occultation: one in the 'X' direction, one in the 'Y' direction. A mean value per day in every direction is calculated and monitored in order to assess instrument performance in terms of star pointing. It can be seen in fig. 4-5.1 that the SATU NEA has been nominal during September with no values out of the thresholds (2 and 3 micro radians in 'X' and 'Y' directions respectively). The results for some occultations belonging to previous months (monthly averages) are presented in fig. 4.5-2, where no trend is visible so far.
Before May 2003, data above 90 km have been considered (instead of 105 km) but from May 2003 on data taken in the mesospheric oxygen layer (located around 100 km altitude) have been avoided because they could cause fluctuations on the SATU data. Also the products with errors (error flag set) are discarded from May 2003 onwards.

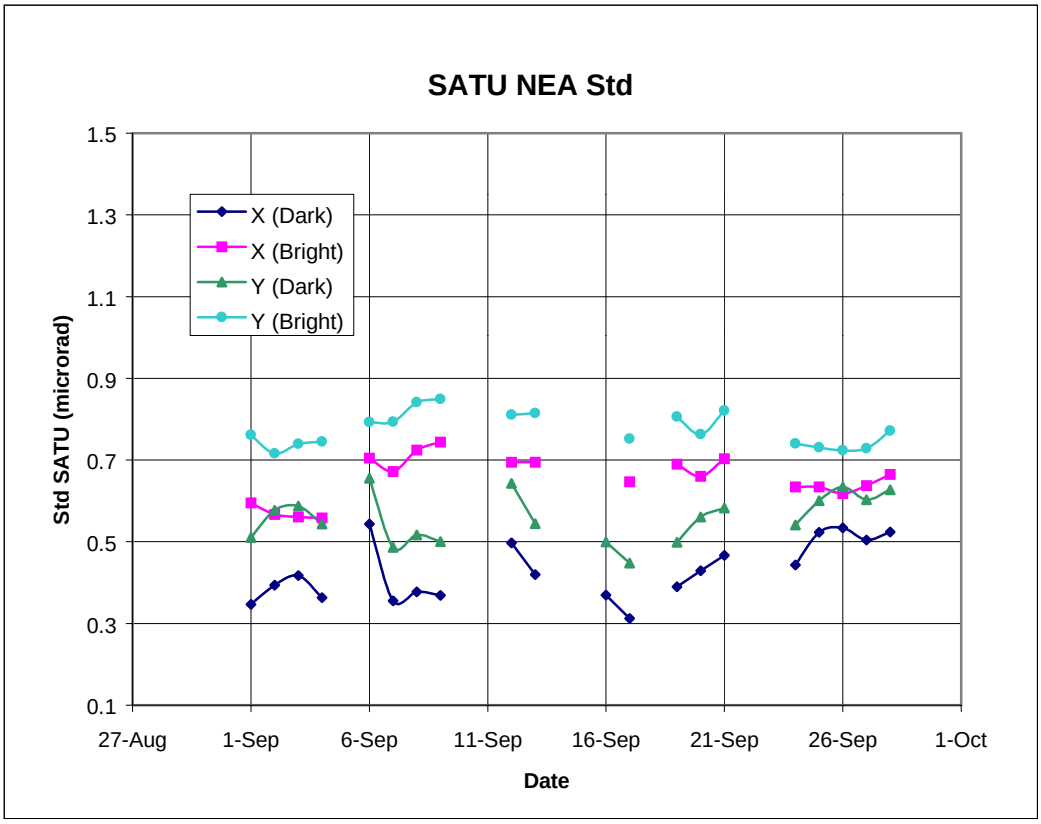

Figure 4.5-1: Average value per day of SATU NEA std above 105 kms

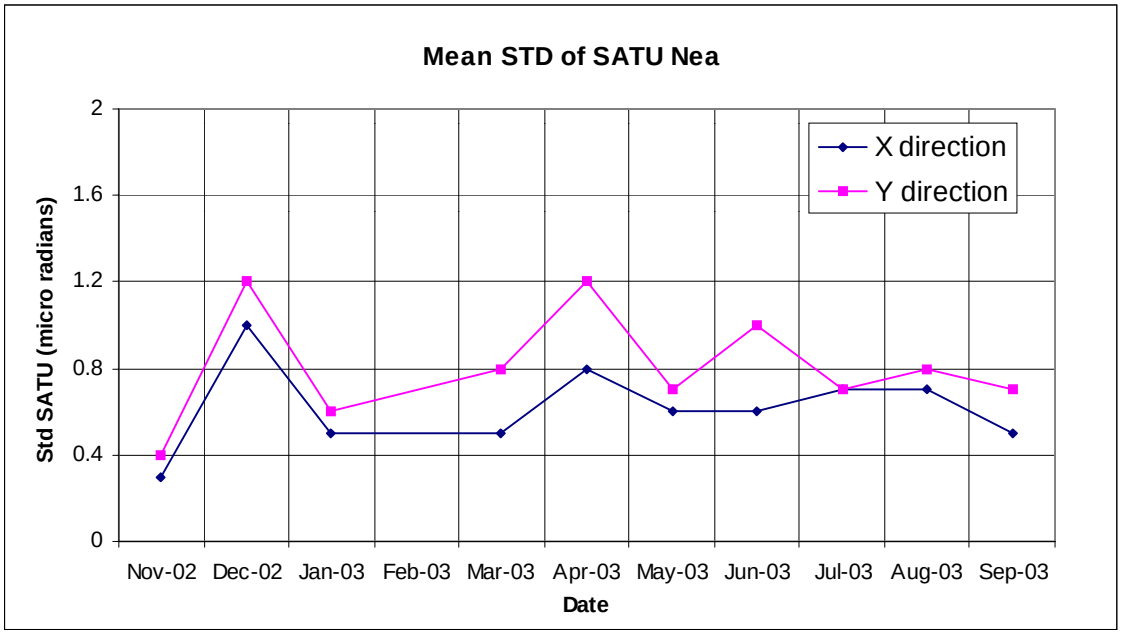

Figure 4.5-2: Average value per month of SATU NEA std above 105 kms

4.5.2 TRACKING LOSS INFORMATION

This verification consists of the monitoring of the tangent altitude at which the star is lost. It is an indicator of the pointing performance although it is to be considered that star tracking is also lost due to the presence of clouds and hence not only due to deficiencies in the pointing performance. Therefore, only the detection of any systematic long-term trend is the main purpose of this monitoring. The recent results are presented in fig. 4.5-3 and fig. 4.5-4:

- The dependence of the altitude at which tracking is lost on the magnitude of the star is very weak because the tracking is mainly lost due to the refraction and the scintillation that depend on the atmospheric conditions.
- The stars lost at high altitude in fig. 4.5-3 belong to very long lasting occultations (very oblique ones) so it is not a fact related to deficiencies in pointing. The other three outliers in the same plot belong to occultations of the star id 63 (twice) and 84.
- In fig. 4.5-4 there is one occultation where the star is lost at high altitude and corresponds to star id 154.
- Some statistics are given in table 4.5-1 calculated for a set of data and not for the whole months.

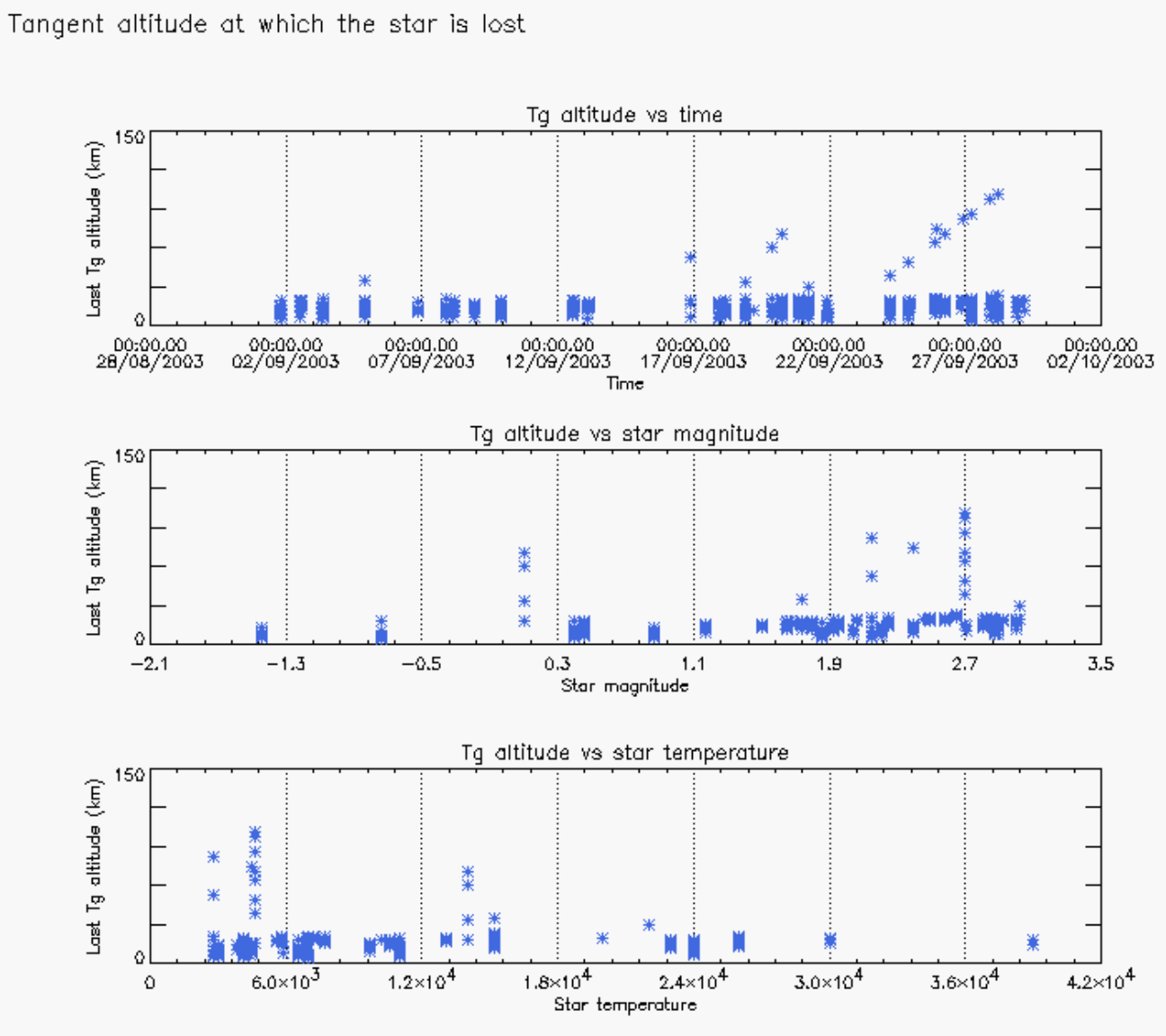

Figure 4.5-3: Last tangent altitude of the occultation (dark limb), point at which the star is lost

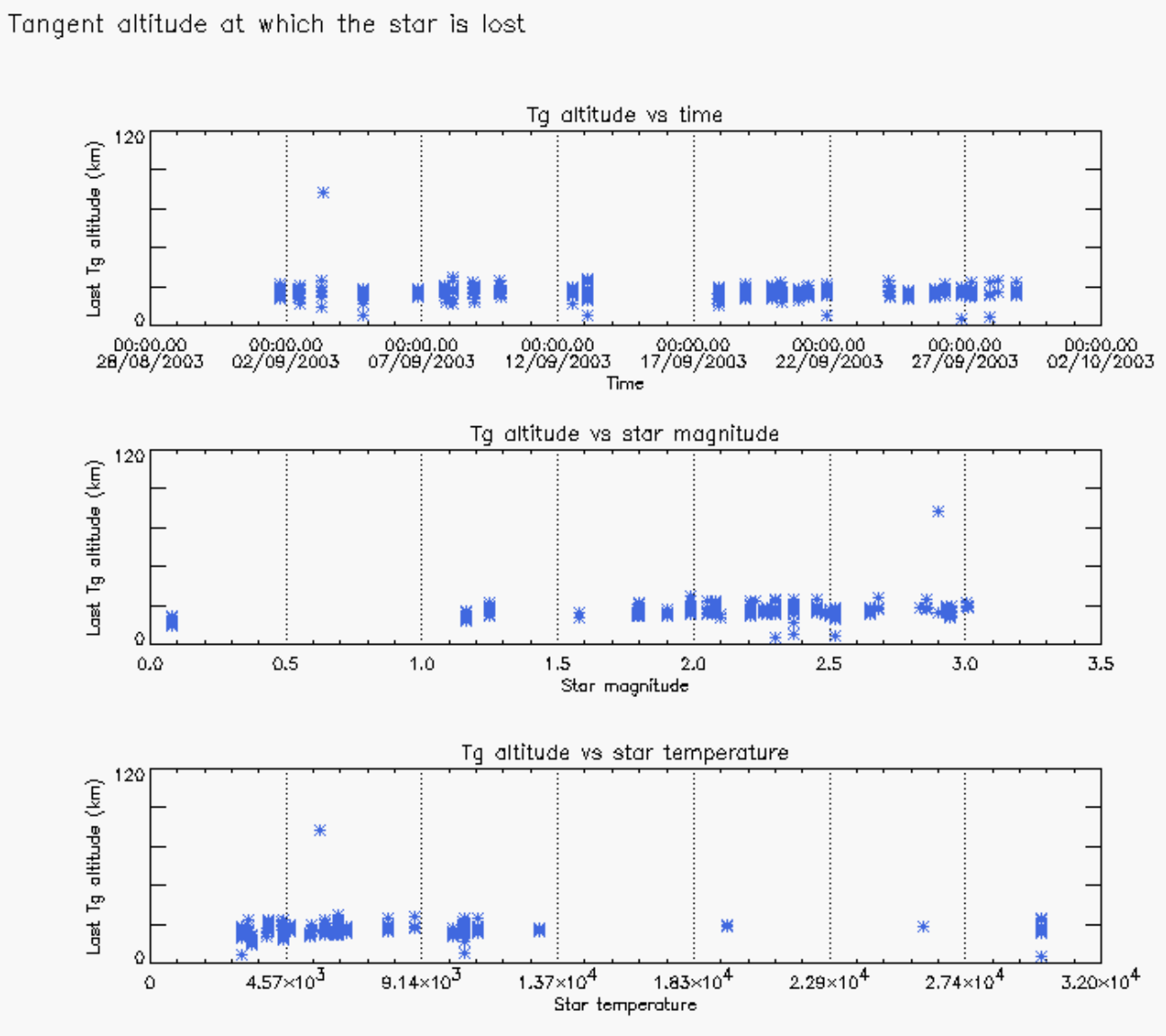

Figure 4.5-4: Last tangent altitude of the occultation (bright limb), point at which the star is lost

Table 4.5-1: Mean tangent altitude (and Std) at which the star is lost for some occultations since January 2003

	Dark limb		Bright limb	
	Mean tg altitude	***Std tg altitude***	***Mean tg altitude***	***Std of tg altitude***
January 2003	15.2	10.4	19.1	7
February 2003	-	-	-	-
March 2003	14.8	9.7	21.3	2.5
April 2003	14.6	9.9	20.7	9.5
May 2003	14.2	2.6	20.3	2.4
June 2003	15.9	7.9	22.4	6.6
July 2003	15.3	6.8	20.3	3.6
August 2003	15.1	7.1	20.8	3.4
September 2003	15.6	11.9	20.5	5.0

4.5.3 MIP (MOST ILLUMINATED PIXEL)

The MIP (Most Illuminated Pixel) is the star position on the SATU CCD in detection mode and it is recorded in the housekeeping data. The nominal centre of the SATU is pixel number **145** in elevation and number **205** in azimuth. The detection of the stars should not be far from this centre. As can be seen in fig. 4.5-5 the azimuth is always well within the threshold (table 4.5-2) since September 2002 even if a small variation is present. The elevation MIP has a significant variation and now the stars are detected a several pixels above the SATU centre. The variation in MIP positions seems to be seasonal and it is an indicator of deviations from expected ENVISAT platform attitude. A mispointing of 0.1 degrees corresponds to a MIP variation onto the SATU CCD of 50 pixels. The MIP displacement will be carefully monitored. Fig. 4.5-6 shows the standard deviation of azimuth and elevation that should be within the thresholds of table 4.5-2.

Table 4.5-2: MIP thresholds

MIP X: mean delta Az	[198 - 210]
Std delta Az	7
MIP Y: mean delta El	[145 – 154]
Std delta El	4

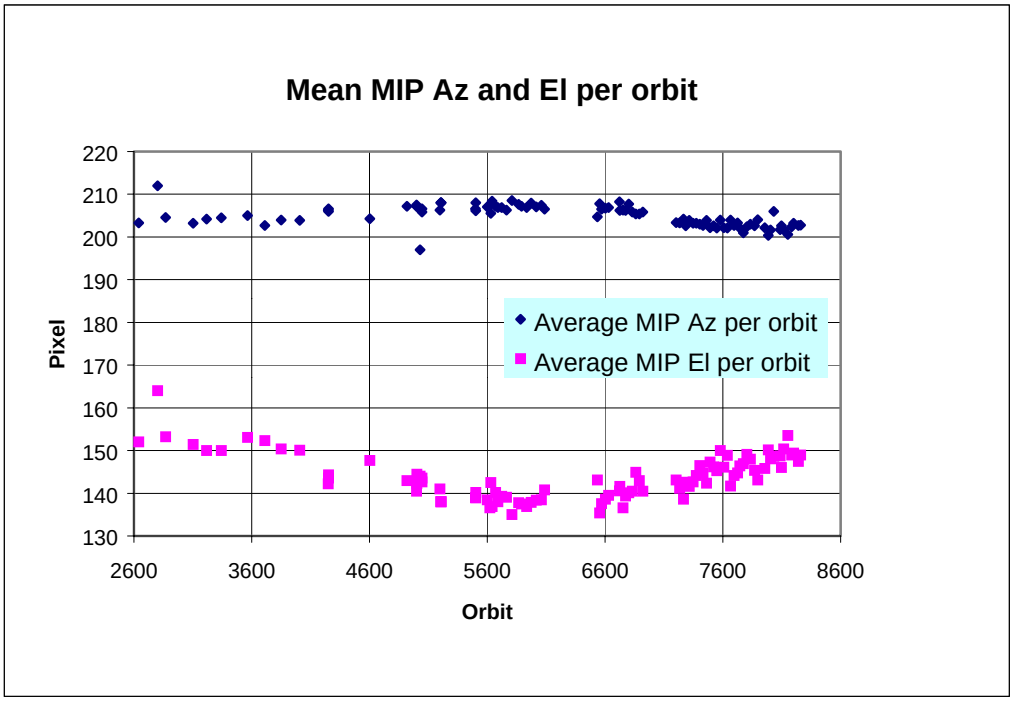

Figure 4.5-5: Mean values of MIP for some orbits since 1st September 2002 (see table 4.5-3)

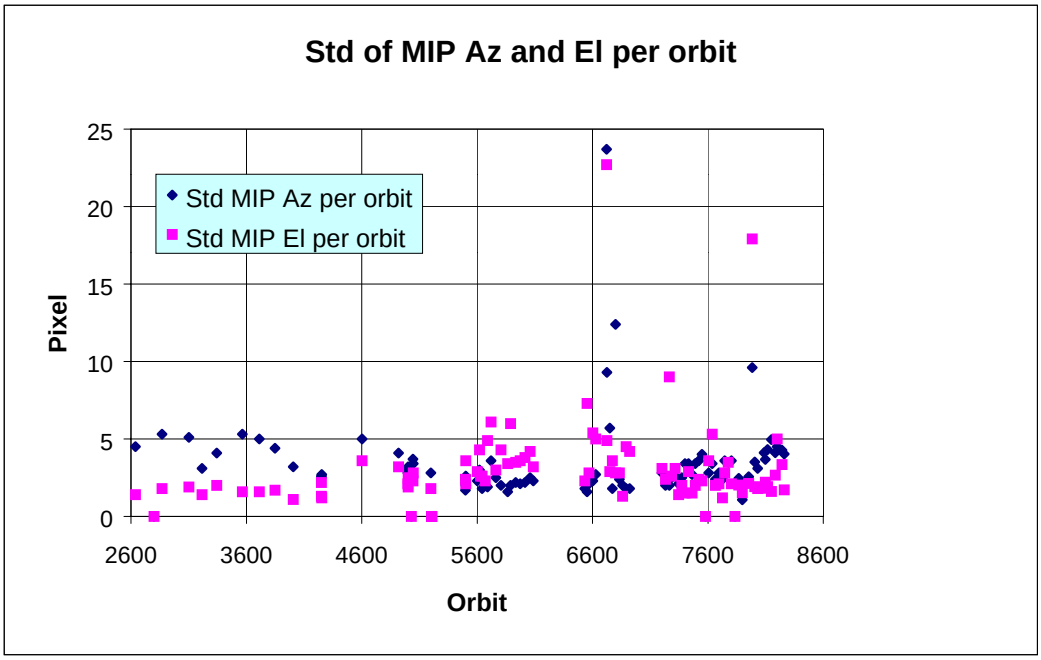

Figure 4.5-6: Standard deviation of MIP Azimuth and Elevation for some orbits since 1st September 2002 (see table 4.5-2)

5 LEVEL 1 PRODUCT QUALITY MONITORING

5.1 Processor Configuration

5.1.1 VERSION

No level 1 products from the PDS have been disseminated to the users in September. About 7% of GOM_TRA_1P products have been received in the PCF for routine quality control and long term trend monitoring. The current level 1 processor software version for the operational ground segment is GOMOS/4.00 (see table 5.1-1) and the product specification is PO-RS-MDA-GS2009_10_3H. This processor has been cleared for initial level 1 data release, with a disclaimer for known artefacts that are currently being resolved and will be implemented in the next release.
http://envisat.esa.int/dataproducts/availability

Table 5.1-1: PDS level 1b product version and main modifications implemented

Date	Version	Description of changes
31-MAY-2003	Level 1b version 4.00 at PDHS-E and PDHS-K	Algorithm baseline level 1b DPM 5.4: • Modulation correction step added after the cosmic rays detection processing • Inversion of the non-linearity and offset corrections • Modification of the computation of the estimated background signal measured by the photometers: use the spectrometer radiometric sensitivity curve and the photometer transfer function. • Use of the dark charge map at orbit level computed from the DSA (dark sky area) if any in the level 0 product • Implementation of a new unfolding algorithm for the photometer samples • See ref. [2] for more details
21-NOV-2002	Level 1b version 3.61 at PDHS-E and PDHS-K	Algorithm baseline DPM 5.3: • Review of some default values • New definition of one PCD flag (atmosphere) • Temporal interpolation of ECMWF data • See ref. [2] for more details

Cal/Val teams are supplied with selected data sets generated by the prototype processor GOPR 5.4. See table 5.1-2 for the prototype level 1b versions and modifications.

Table 5.1-2: GOPR level 1b product version and main modifications implemented

Date	Version	Description of changes
17-MAR-2003	GOPR 5.4c	• Modification of the CAL ADFs (update of the limb radiometric LUT). The products are affected only if the limb spectra are converted into physical units • Modifications to allow compatibility with ACRI computational cluster (no modifications of the results) • Modification of the logic to handle dark charge map refresh at orbit level (DSA data is now directly processed by the level 1b processor if available in the level 0 product). No impact on the results
21-FEB-2003	GOPR 5.4b	• DC map values are rounded when written in the level 1b product • Modification of the CAL ADFs (update of the wavelength assignment of SPB1 and SPB2) • Modify the computation of flag_mod in the modulation correction routine
17-JAN-2003	GOPR 5.4a	• use the start and stop dates of the occultation when calling the CFI interpol instead of start and stop dates of the level 0 product • modify the ECMWF filename information in the SPH of the level 1b and limb products

5.1.2 AUXILIARY DATA FILES (ADF)

The ADF's files in table 5.1-2 are used by the PDS to process the data from level 0 to level 1. For every type of file, the validity runs from the start validity time until the start validity time of the following one. On 9th, 19th and 29th September new calibration ADF's were disseminated with updated DC map of orbits 07955, 08111 and 08253 respectively.

Table 5.1-3: Level 1b ADF's for September 2003

Filename	Validity time	Dissemination time
GOM_CAL_AXVIEC20030929_143746_20030926_000000_20100101_000000	26-SEP-2003	29-SEP-2003
GOM_CAL_AXVIEC20030919_100831_20030916_000000_20100101_000000	16-SEP-2003→25-SEP-2003	19-SEP-2003
GOM_CAL_AXVIEC20030909_134320_20030904_000000_20100101_000000	04-SEP-2003→15-SEP-2003	09-SEP-2003
GOM_CAL_AXVIEC20030827_090357_20030825_000000_20100101_000000	25-AUG-2003→03-SEP-2003	27-AUG-2003
GOM_INS_AXVIEC20030716_105425_20030716_120000_20100101_000000	16-JUL-2003	16-JUL-2003
GOM_PR1_AXVIEC20030326_085805_20020324_200000_20100101_000000	24-MAR-2002	26-MAR-2003
GOM_STS_AXVIEC20020121_165822_20020101_000000_20200101_000000	01-JAN-2002	21-JAN-2002
GOM_CAT_AXIEC20020121_161009_20020101_000000_20200101_000000	01-MAR-2002	21-JAN-2002

5.2 Quality Flags monitoring

In this section it is monitored some Product Quality information stored in the level 1b products. On the one hand, for every product we have information of the **number of measurements** where a given problem was detected (i.e. number of invalid measurements, number of measurements containing saturated samples, number of measurements with demodulation flag set…). On the other hand, there are **flags** that indicate problems within the product (i.e. flag set to one if the reference spectrum was computed from DB, flag set to zero if SATU data were not used…).

For the information on the number of measurements a plot (percentages) is provided in fig. 5.2-1. It can be seen that the cosmic rays hits occurred often for the 95% of the measurements of the product. Another observation that can be done is that, for many products, the 30 % of the measurements have the star signal falling outside the central band.

The flag information is given in table 5.2-1. It is reported also the percentage of the products that have at least one measurement with demodulation flag set.

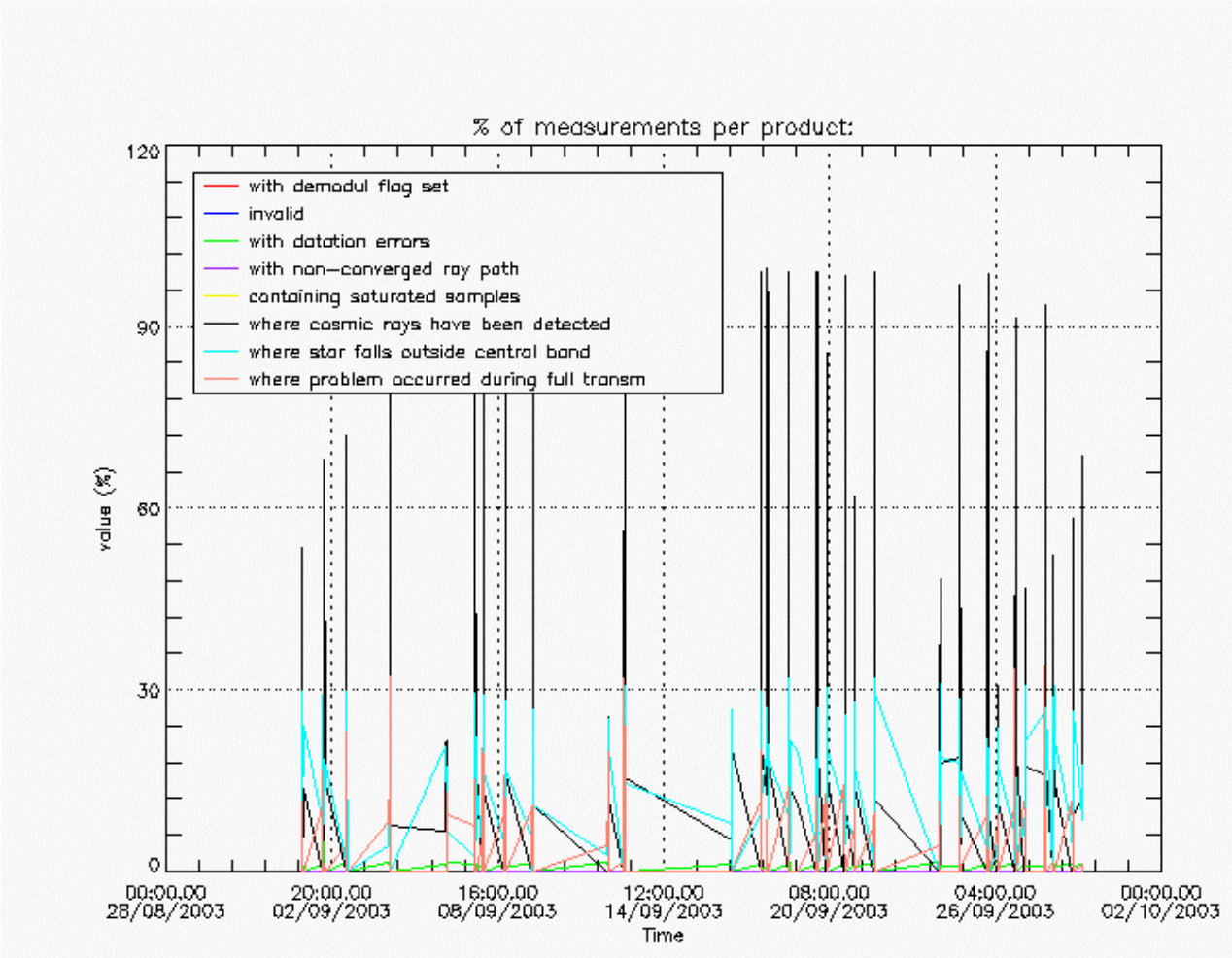

Figure 5.2-1: Level 1b product quality monitoring

Table 5.2-1: Percentage of products during the reporting period with:

At least one measurement with demodulation flag set:	11.2654 %
Reference spectrum computed from DB:	0.00000 %
Reference spectrum with small number of measurements:	0.00000 %
SATU data not used:	0.00000 %

5.3 Spectral Performance

No new spectral calibration has been done during September. These results were already presented in previous versions of the MR with nominal results thus far.

The values reported (table 5.3-1) are, for every star ID (1, 2, 4, 9, 18, 25), the wavelength of the first useful pixel of SPA2. This value is calculated by addition to the actual wavelength assignment, the spectral shift for which a maximum correlation has been found between the reference spectrum and the one of the occultation. It can be observed in table 5.3-1 that for all the stars (but for star id 4) the

difference between the actual wavelength (690.492981 nm) and the one reported in the table is between –0.06 and 0.05 nm. Thus, the wavelength has not been updated in the Calibration product. It is foreseen not to use the star id 4 for wavelength calibration purposes.

Table 5.3-1: New wavelength assignment calculated for several occultations since November 2002.

Star ID / Level 0 date	1	2	4	9	18	25
20021112_062935	Occ.30: 690.455750	Occ.26: 690.458740		Occ.28: 690.492981		
20021219_102754		Occ.33: 690.468140	Occ.26: 690.875122			
20030101_151630	Occ.3: 690.445068	Occ.37: 690.466003	Occ.30: 690.878540			
20030110_121504		Occ.32: 690.465088	Occ.25: 690.882385			
20030201_090221						Occ.21: 690.492981
20030415_123156			Occ.29: 690.959534		Occ.20: 690.552002	Occ.28: 690.492981
20030419_170041			Occ.29: 690.957520		Occ.23: 690.555420	
20030428_072600					Occ.19: 690.553645	Occ.28: 690. 492981
20030717_053233				Occ. 22: 690.473816	Occ. 26: 690.446594	

5.4 Radiometric Performance

5.4.1 RADIOMETRIC SENSITIVITY

The monitoring performed consists in the calculation of the radiometric sensitivity of each CCD by computing the ratio between parts of the reference spectrum using specific stars. In the plot (fig. 5.4-1) the ratios are normalized. The variation of the ratio should be within a given threshold actually set to 10% (see table 5.4-1). For every star, this variation is calculated as the difference between the maximum (or minimum) ratio, and the mean over the 15 first values (if there are not 15 values computed yet, all values are used). Values outside the warning threshold of 10% are now observed, and investigation results will be reported in future monthly reports.

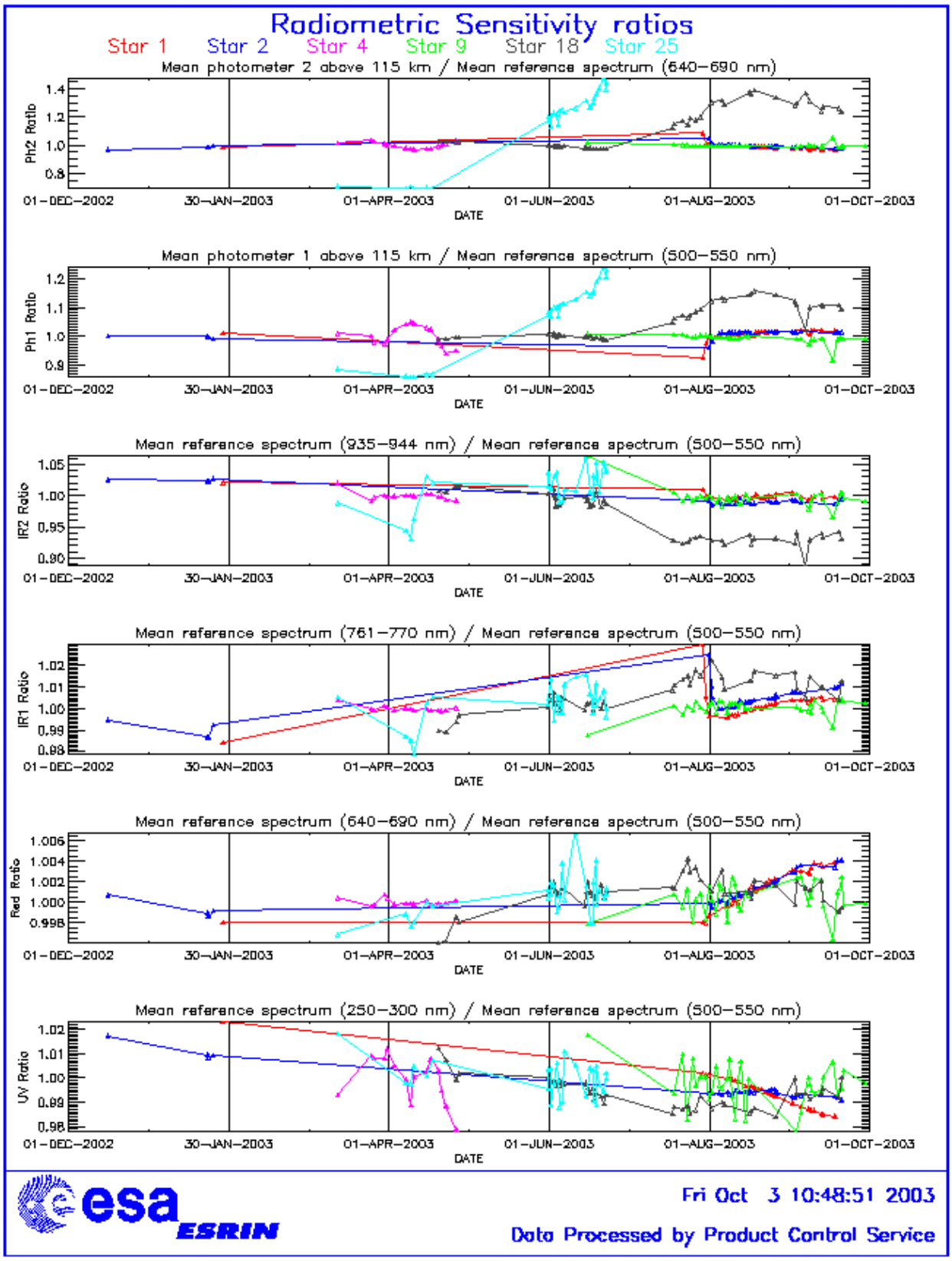

Figure 5.4-1: Radiometric Sensitivity ratios.

Table 5.4-1: Variation of RS for the different ratios. Should be less than 10%.

Star Id	% variation of UV ratio	% variation of Red ratio	% variation of IR1 ratio	% variation of IR2 ratio	% variation of Ph1 ratio	% variation of Ph2 ratio
1	0.503138	0.135869	0.387800	0.0967972	4.16760	10.4636
2	0.0926144	0.172892	0.418974	0.180858	2.10667	6.07233
4	0.0529779	0.0468850	0.115433	0.233174	2.51800	4.93374
9	1.65465	0.121760	0.142307	0.233455	4.79555	6.18962
18	0.223948	0.159591	0.319214	0.608099	8.60293	46.4198
25	2.55773	0.212821	0.225987	0.223921	15.9214	78.6219

5.4.2 PIXEL RESPONSE NON UNIFORMITY (PRNU)

No new PRNU calibration has been done during September. During May a new PRNU calibration has been performed and processed into an update of the PRNU maps for the SPB1 and SPB2 that have been included in the auxiliary file GOM_CAL disseminated at the end of June 2003.

5.5 Other Calibration Results

Future reports will address other calibration results, when available.

6 LEVEL 2 PRODUCT QUALITY MONITORING

6.1 Processor Configuration

6.1.1 VERSION

No level 2 products from the operational ground segment have been disseminated during September to the users. About 25% of GOM_NL__2P products have been received in the PCF for routine quality control and long term trend monitoring. The current level 2-processor software version for the operational ground segment is GOMOS/4.00 (see table 6.1-1) and the product specification is PO-RS-MDA-GS2009_10_3H. The improvements defined at the Validation Workshop are currently being implemented into the prototype processor, before implementation into the operational one. In the mean time, Cal/Val teams are supplied with selected data sets generated by the previous prototype processor GOPR 5.4 (see table 6.1-2).

Table 6.1-1: PDS level 2 product version and main modifications implemented

Date	Version	Description of changes
31-MAY-2003	Level 2 version 4.00 at PDHS-E and PDHS-K	Algorithm baseline level 2 DPM 5.4: • Revision of some default values • Add a new parameter • Transmission model computation: suppress tests on valid pixels and species • Apply a Gaussian filter to the vertical inversion matrix • Very low signal values are substituted by threshold value • See ref. [3] for more details
21-NOV-2002	Level 2 version 3.61 at PDHS-E and PDHS-K	Algorithm baseline level 2 DPM 5.3a: • Revision of some default values • Wording of test T11 • Dilution term computation of jend • Covariance computation scaling applied before and after • See ref. [3] for more details

Table 6.1-2: GOPR level 2 product version and main modifications implemented

Date	Version	Description of changes
18-MAR-2003	GOPR 5.4b	• modification to implement the computation of Tmodel for spectrometer B (in version 5.4b, the Tmodel for SPB is still set to 1)
30-JAN-2003	GOPR 5.4a	• modifications for ACRI internal use only. No impact on level 2 products.

6.1.2 AUXILIARY DATA FILES (ADF)

The ADF's files in table 6.1-1 are used by the PDS to process the data from level 1 to level 2. For every type of file, the validity runs from the start validity time until the start validity time of the following one.

Table 6.1-3: Level 2 ADF's for September

Filename	Validity time
GOM_INS_AXVIEC20021112_170146_20020301_000000_20100101_000000	01-MAR-2002
GOM_PR2_AXVIEC20021112_170458_20020301_000000_20100101_000000	01-MAR-2002
GOM_CRS_AXVIEC20020729_082931_20020301_000000_20100101_000000	01-MAR-2002

6.2 Other Level 2 performance issues

The plot presented in fig. 6.2-1 is the average of the Ozone values during September in a grid of 0.5 degrees in latitude per 1 km in altitude. This plot will be compared with the same kind of plot for the following months to detect any major problem and to see how the Ozone evolves from one month to the other.

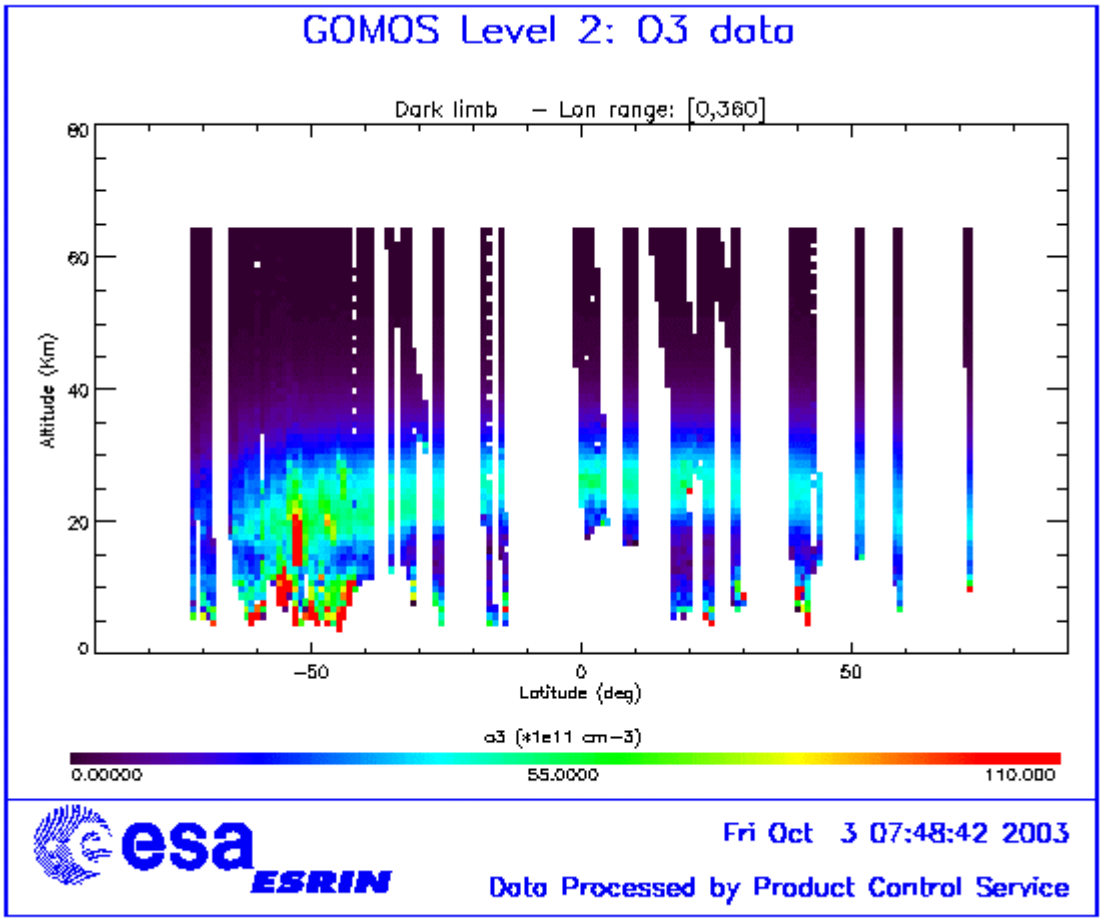

Figure 6.2-1: Average GOMOS O_3 profile during September: average in a grid of 0.5° latitude x 1 Km altitude

7 VALIDATION ACTIVITIES AND RESULTS

7.1 Intercomparison with external data

Comparisons between lidar measurements and GOMOS profiles generated with two versions of level 2 GOPR 5.4 (5.4b and 5.4d) have been done (fig. 7.1-1). The coincidence criterion in distance is 1000 km while in time is 4 hours. In all cases, the amplitude of the averaged median value is reduced when calculated with GOMOS profiles processed with v5.4d instead of GOMOS profiles processed with v5.4b. The mean value of the relative difference is also reduced when calculated with GOMOS profiles processed with v5.4d (table 7.1-1).

***Note**: the major difference between the versions GOPR 5.4b and 5.4d is the implementation of the Tikhonov regularization in the version 5.4d*

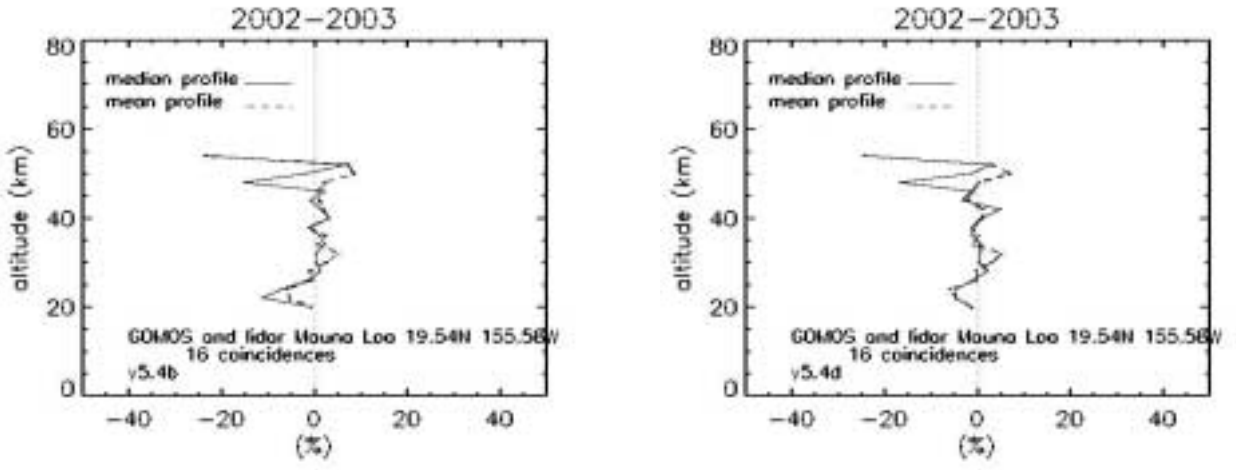

Figure 7.1-1: Comparison GOMOS/lidar measurements at Mauna Loa (Mauna Loa data courtesy of I. Stuart McDermid and Thierry Leblanc from JPL, Table Mountain Facility, California Institute of Technology)

Table 7.1-1: Median and mean values of the relative difference between the GOMOS profiles and the external measurement profiles averaged by altitude layer

	median value v5.4b	**median value v5.4d**	mean value v5.4b	**mean value v5.4d**
lidar at Mauna Loa (20-30km)	-3.70	**-1.85**	-2.65	**-2.35**
lidar at Mauna Loa (30-40km)	0.59	**-0.04**	2.07	**1.37**

7.2 GOMOS-Climatology comparisons

It is focussed on the validation dataset including occultations measured between September 2002 and June 2003 and whose level 2 products were processed with 2 different versions of the GOMOS prototype: v5.4b and v5.4d. The comparison of the O_3 vertical profiles processed with the 2 versions allows a first assessment of the expected improvement on the profiles generated with the version v5.4d. This validation dataset includes more than 2300 dark occultations processed with both versions, measured during the following months: September 2002, December 2002, January 2003, April 2003, May 2003 and June 2003.

It is presented the results of the comparison of O_3 profiles with the Fortuyn-Kelder climatology at different pressure levels for a few latitude bands, using GOMOS profiles generated with the two versions of the level 2 processor. For the 3 latitude bands presented (fig. 7.2-1, 7.2-2, 7.3-3, 7.2-4, 7.2-5, 7.3-6), the variability of the difference between GOMOS O_3 concentration values and the climatological values is lower for most of the profiles if calculated with the v5.4d version instead of the v5.4b version (30hPa, 5hPa, 3hPa at 5°S-5°N; 30hPa at 15°N-25°N…). Moreover, in some cases, the values of the difference are closer to zero with the most recent processing version (30hPa, 20hPa at 45°S-35°S). For only a few measurements, the difference with the climatology is larger in amplitude than with the old version at the lowest pressure level (0.3hPa at 45°S-35°S, 0.3hPa at 15°N-25°N).

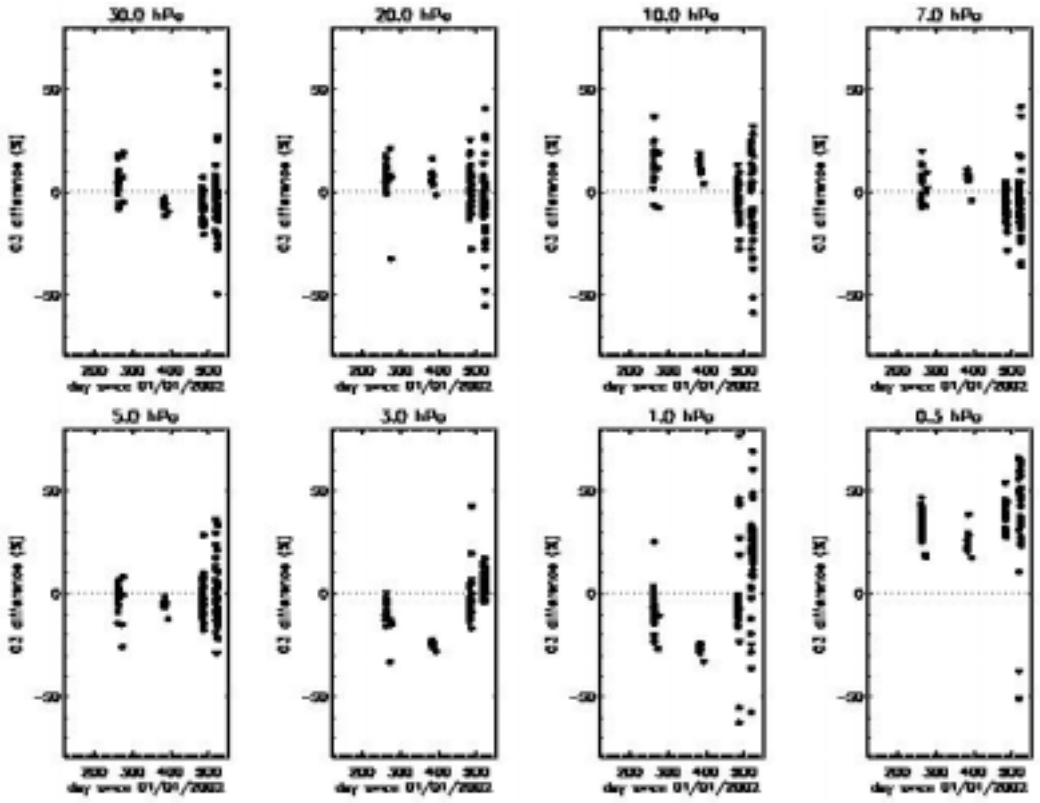

Figure 7.2-1: **Comparison with Fortuyn and Kelder climatology version v5.4b (45°S-35°S)**

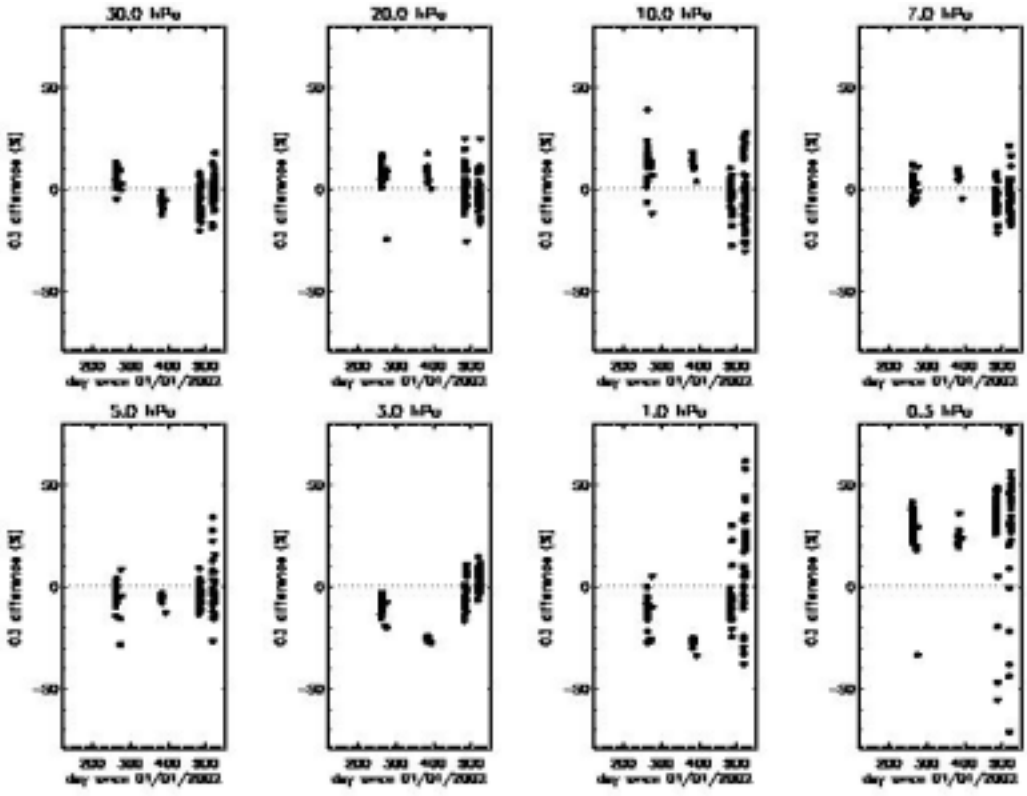

Figure 7.2-2: Comparison with Fortuyn and Kelder climatology, version v5.4d (45°S-35°S)

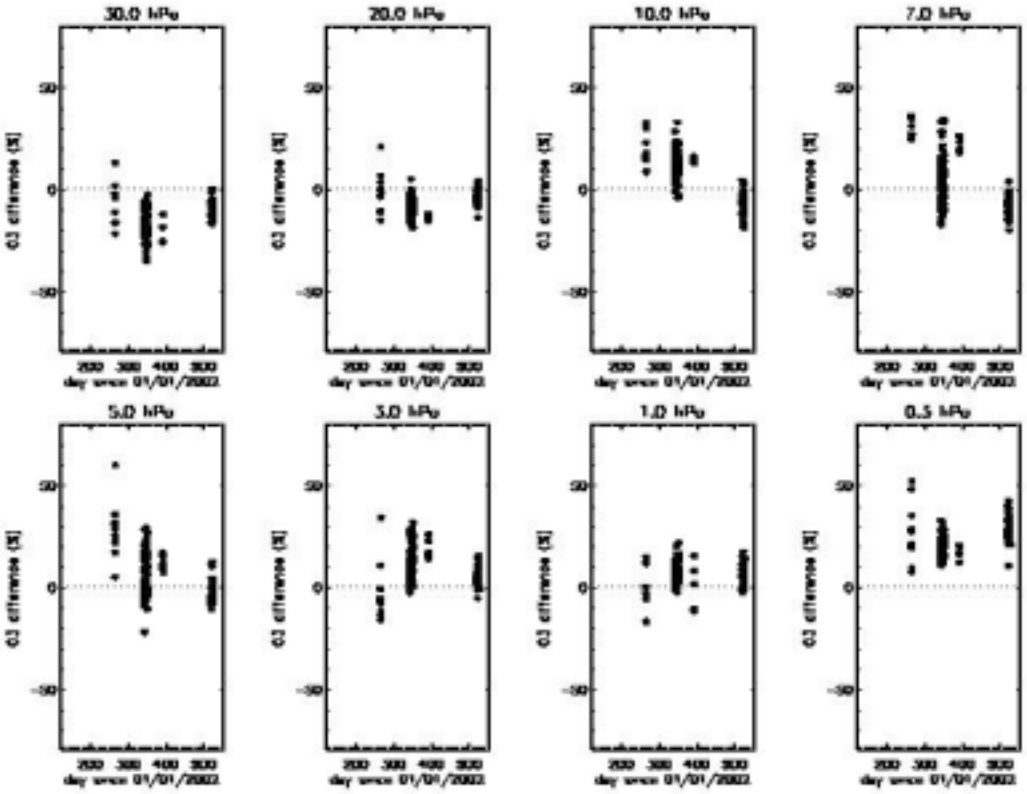

Figure 7.2-3: Comparison with Fortuyn and Kelder climatology, version v5.4b (5°S-5°N)

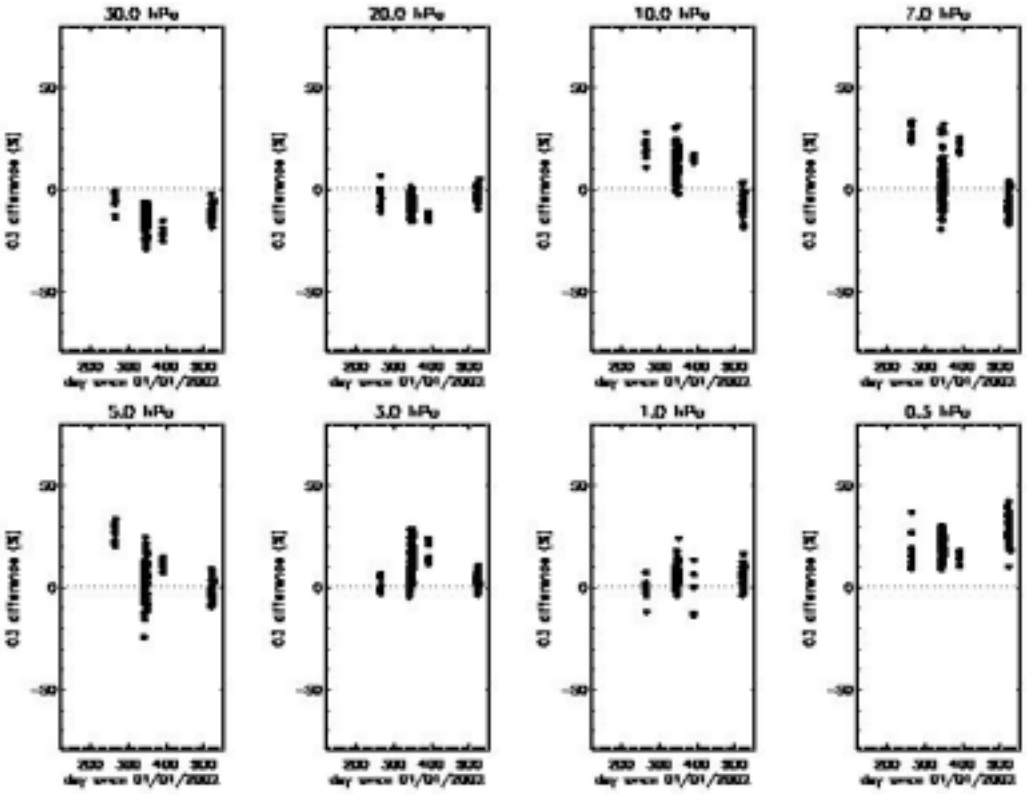

Figure 7.2-4: Comparison with Fortuyn and Kelder climatology, version v5.4d (5°S-5°N)

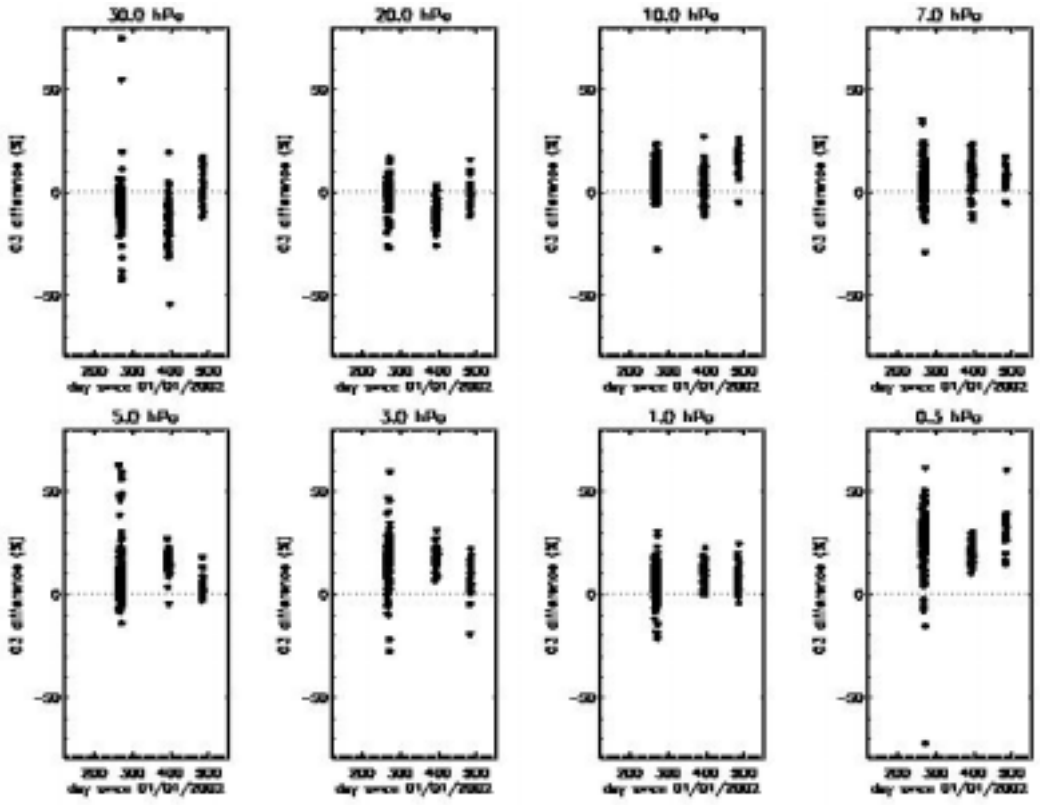

Figure 7.2-5: Comparison with Fortuyn and Kelder climatology, version v5.4b (15°N-25°N)

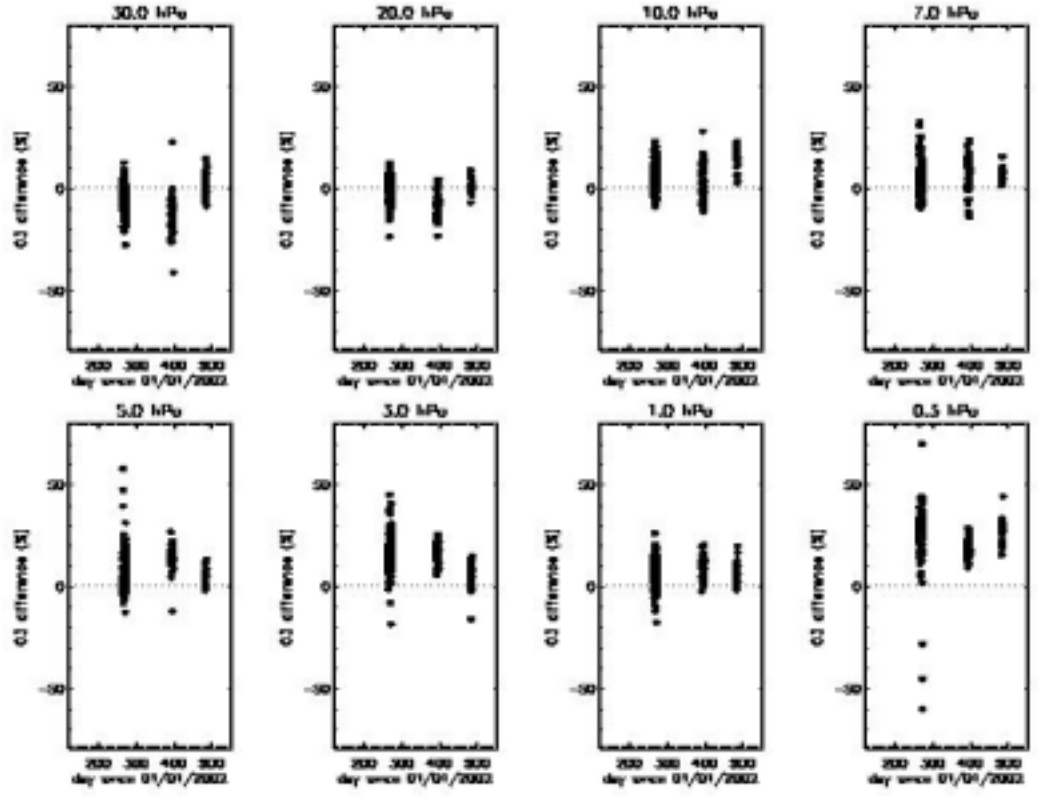

Figure 7.2-6: Comparison with Fortuyn and Kelder climatology, version v5.4d (15°N-25°N)

7.3 GOMOS Assimilation with MSDOL

MSDOL is a system tool able to assimilate GOMOS data for the production of a three-dimensional time series model of the distribution of ozone and other trace gases. An assimilation experiment using the newly available GOMOS level2 products v5.4d has been conducted. Ozone local densities profiles have been assimilated in the model initialised on August 1st, 2003 and running for more than one month.

A comparison has been performed with the balloon ozone soundings performed from the Antarctic ground station Marambio (56.72°W, 64.23°S) available on the NILU CAL/VAL database. This thus focused on the lowermost part of the stratosphere, as balloon soundings never exceed 35 km altitude. The fig. 7.3-1 shows the ozone partial pressure over Marambio as a function of time (in abscissa, ranging from Aug 1st to Sep 8th) and of geopotential altitude. The vertical bars between the ground and about 30 km altitude show the values measured by the balloon soundings.

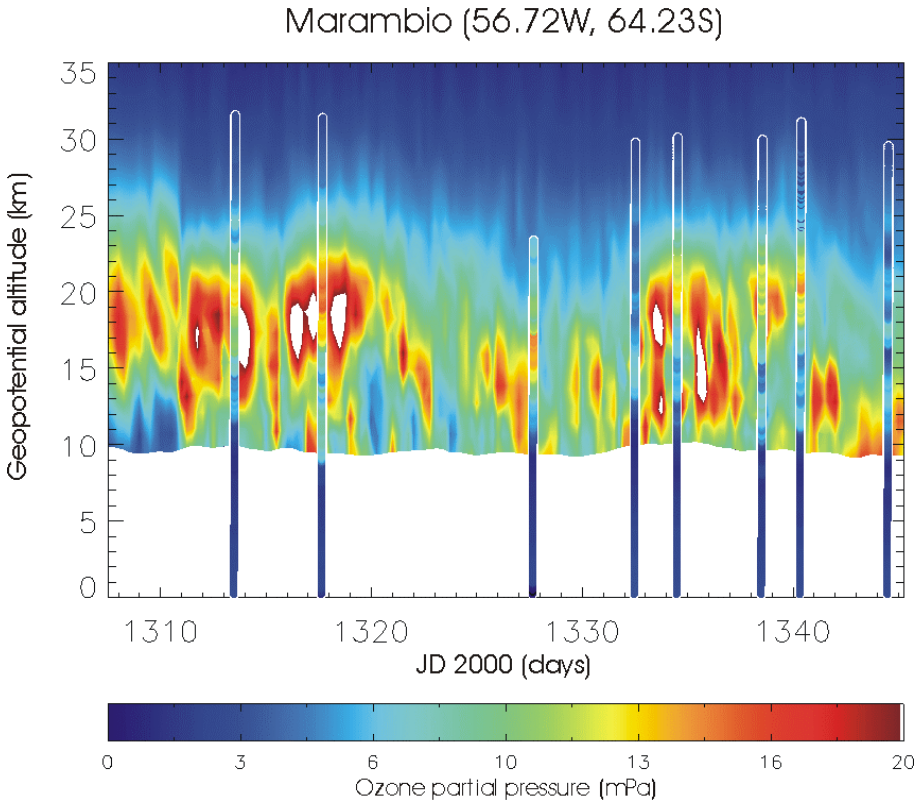

Figure 7.3-1: Ozone partial pressure over Marambio as a function of time (Marambio data courtesy of Juha A. Karhu from FMI and Maximo Ginzburg from SMNA)

It can be seen that while the agreement between the assimilated ozone field and the ground-based soundings is quite good above 25 km altitude, the assimilated ozone field exhibits high peaks of ozone in the region 10-25 km. These are probably “data shocks” caused by the assimilation process. The variability of GOMOS measurements in that region is indeed quite high, and there are still oscillations or outliers in version 5.4d. This is apparent in fig. 7.3-2 in which are plotted GOMOS profiles closest to Marambio during the whole period. The colour scale simply indicates the date at which the measurement was performed (from blue to red).

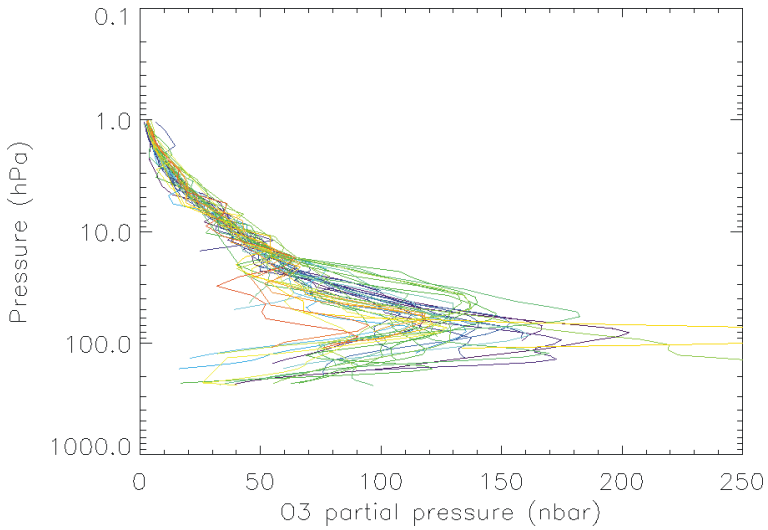

Figure 7.3-2: GOMOS profiles near Marambio during assimilation period

The fig. 7.3-3 shows a scatter plot of the quantities “Observation minus Analysis” (OmA) versus “Observation minus Forecast” (OmF). If a point lies on the diagonal, it means that the assimilation had no effect; on the other hand, a point lying on the horizontal indicates that assimilation resulted in the analysis being driven to the observations without taking the forecast into account. One can see that the assimilation performed well as the points lie in between these two lines. The colour scale is indicative of the altitude of the measurement (red is the lower). There is however no clear pattern emerging, the points being rather equally distributed.

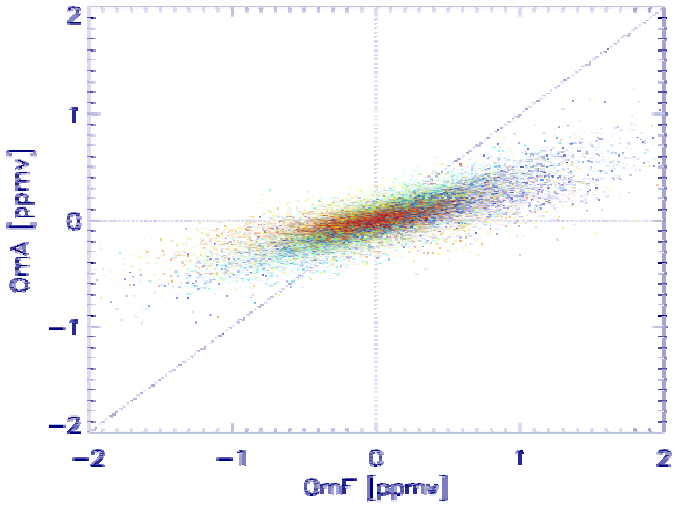

Figure 7.3-3: Observation minus Analysis vs Observation minus forecast

The time evolution of these quantities is also shown (fig. 7.3-4). Again, the colour scale is related to the altitude of the measurement. Clearly apparent is the lessening of the variability of the series after assimilation: the analysis is closer to the observations that the forecast indicating again that the assimilation performs well. However, it does not seem there is an attenuation of the standard deviation of the OmF with time as measurements are assimilated into the model.

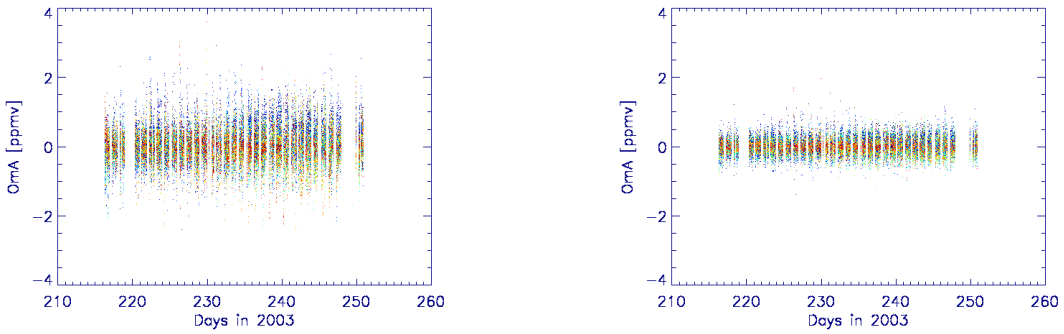

Figure 7.3-4: Time evolutions of OmF (left). Time evolution of OmA (right)

It is interesting to look at the same plot but for thinner layers. It has been arbitrarily chosen to use Umkher layers to discretize the atmosphere. In fig. 7.3-5 it is plotted the time evolution of the OmF (left) and OmA (right) for Umkher layer 8 (top, middle stratosphere) and 2 (bottom, lower stratosphere). There is a striking high variability of the OmF in Umkher layer 8, along with a clearly visible drift of the mean value. This is however well corrected by the assimilation process, but this phenomenon has to be investigated further. This is however not visible in Umkher layer 2.

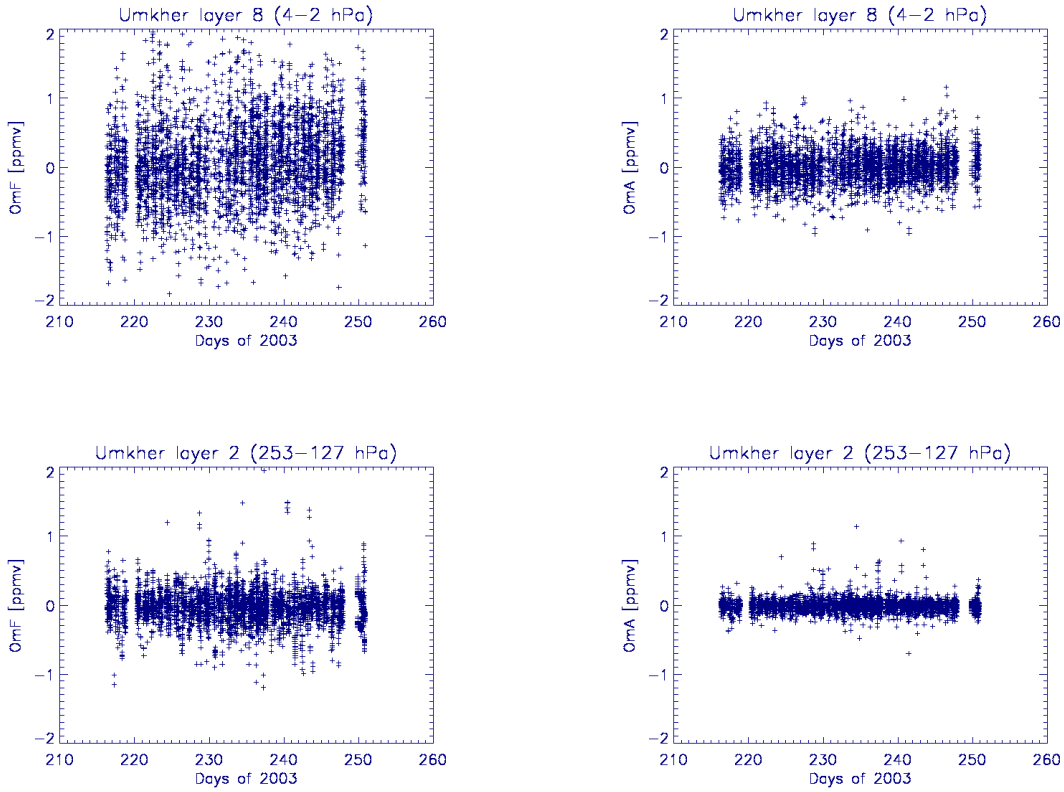

Figure 7.3-5: Time evolution of: OmF layer 8 (left top), OmF layer 2 (left bottom), OmA layer 8 (right top), OmA layer 2 (right bottom)

Fig. 7.3-6 shows the correction on the ozone field that is the quantity “Analysis minus Forecast” for Umkher layer 2. No clear pattern emerges, indicating that this quantity is roughly normally distributed which can be verified by plotting its histogram (fig. 7.3-7) where a slight bias is observed.

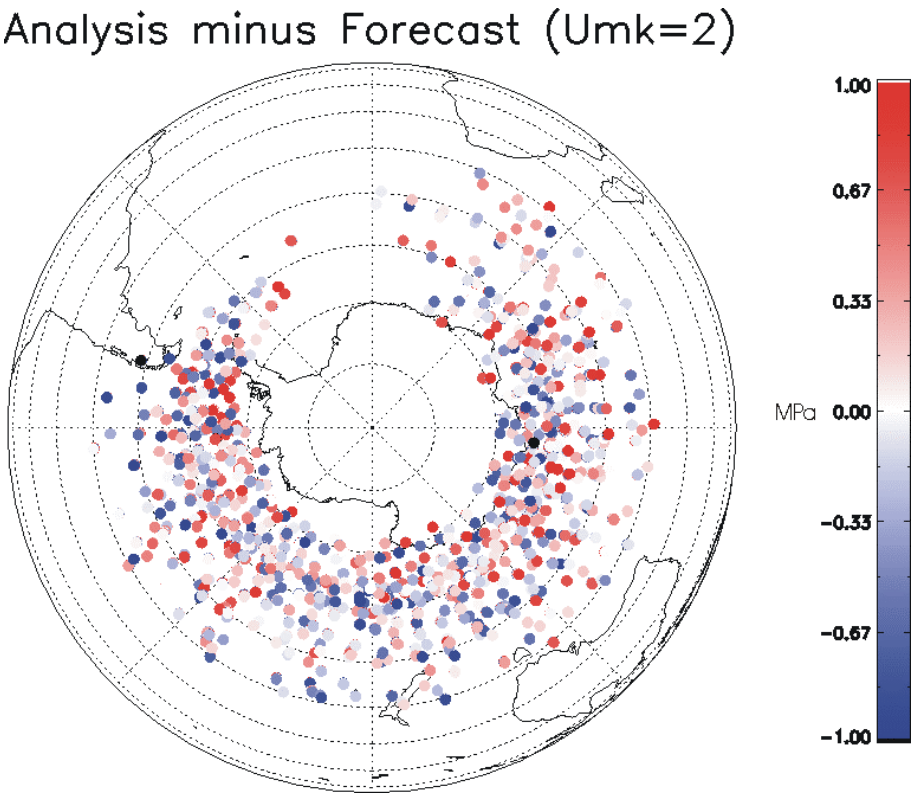

Figure 7.3-6: Analysis minus Forecast for Umkher layer 2

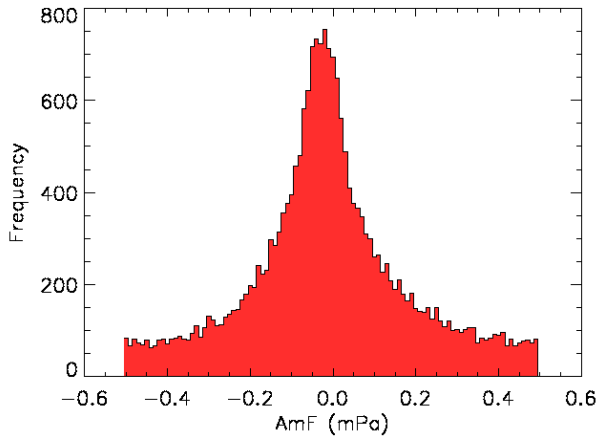

Figure 7.3-7: Histogram of Analysis minus Forecast for Umkher layer 2

The quantity OmF can be used to gain insight into the precision of GOMOS measurements. As an illustration, the table 7.3-1 gives the value of the standard deviation of the OmF series for each Umkher layer, normalized to the mean value of the ozone at that level. The corresponding percentage gives a rough estimate of the GOMOS measurements error for that layer, at least with respect to the model. It can be seen that it is noticeably higher than the value written in the product. Of course, this should be amended by taking into account that several stars, yielding different accuracies, have been observed.

Table 7.3-1: Standard deviation of OmF series for different Umkher layer

Umkher layer	pmax	pmin	σ(OmF)[ppmv]	<O3> [ppmv]	σ/<O3> [%]
2	253.312	126.656	0.246392	0.515083	47.8355
3	126.656	63.3281	0.415955	1.38168	30.1051
4	63.3281	31.6641	0.512510	2.96816	17.2669
5	31.6641	15.8320	0.412376	4.18674	9.84959
6	15.8320	7.91602	0.483766	5.17039	9.35646
7	7.91602	3.95801	0.471038	5.83230	8.07636
8	3.95801	1.97900	0.585835	5.19575	11.2753
9	1.97900	0.989502	0.553078	3.91873	14.1137

7.4 Consistency Verification: GOMOS-GOMOS intercomparison

Future reports will report on this upon availability.